DELIVERABLE D3.10
SUMMARY OF CHEMICAL AND PHYSICAL TESTS FOR COLDER REINJECTION

WP3: Upscaling of thermal power production and optimized operation of EGS plants

Contractual delivery date:	M41
Actual delivery date:	M41

PROJECT INFORMATION

Grant Agreement n°	792037
Dates	1st May 2018 – 31 January 2022

This project has received funding from the European Union's Horizon 2020 research and innovation programme under grant agreement No 792037

DOCUMENT INFORMATION

Version	VF	**Dissemination level**	PU
Editor	ELEONORE DALMAIS (ESG)		
Other authors	CAMILLE JESTIN (FEBUS OPTICS), VINCENT MAURER (ESG), PIERCE KUNAN (ESG)		

DOCUMENT APPROVAL

Name	Position in project	Organisation	Date	Visa
ALBERT GENTER	Project Coordinator	ES GEOTHERMIE	29/09/2021	OK
ELEONORE DALMAIS	WP Leader	ES GEOTHERMIE	29/09/2021	OK
JEAN HERISSON	Project Manager Officer	AYMING	29/09/2021	OK
RONAN HEBERT	Internal Reviewer	CYU	29/09/2021	OK

DOCUMENT HISTORY

Version	Date	Modifications	Authors
V1	29/09/2021	ToC	DALMAIS E / ESG
VF	29/09/2021	Final checks	HERISSON J / Ayming

CONTENT

LIST OF FIGURES

LIST OF TABLES

PUBLIC SUMMARY

The objective of Work Package 3 of MEET project is to assess the feasibility to lower the reinjection temperature on EGS plant in the Upper Rhine Graben from 70°C down to 40°C. This colder reinjection would allow to valorise more energy with the same facilities.

This report compiles physical and chemical measurements acquired while performing different on-site tests for colder reinjection. The demo-site consists in the EGS power plant of Soultz-sous-Forêts (France). Two colder reinjection tests were performed on this site: one with a small heat exchanger to study scaling precipitation down to 40°C and assess the behaviour of different metallurgies and the other one to test the production of electricity at these low temperatures with a small mobile Organic Rankine Cycle (ORC) unit.

This report presents in a first part the geochemical measurements performed on scales for the first test together with a geochemical modelling to better understand the trigging factors of such phenomena. Then, in a second part, the results of reservoir and environment monitoring during the mobile ORC test are presented and discussed.

1 EXECUTIVE SUMMARY

1.1 DESCRIPTION OF THE DELIVERABLE CONTENT AND PURPOSE

The objective of Work Package 3 of MEET project is to assess the feasibility to lower the reinjection temperature on EGS plant in the Upper Rhine Graben from 70°C down to 40°C. This colder reinjection would allow to valorise more energy with the same facilities.

This report compiles physical and chemical measurements acquired while performing different on-site tests for colder reinjection. The demo-site consists in the EGS power plant of Soultz-sous-Forêts (France). 2 colder reinjection tests were performed on this site: one with a small heat exchanger to study scaling precipitation down to 40°C and assess the behaviour of different metallurgies and the other one to test the production of electricity at these low temperatures with a small mobile Organic Rankine Cycle (ORC) unit.

This report presents in a first part the geochemical measurements performed on scales for the first test together with a geochemical modelling to better understand the trigging factors of such phenomena. Then, in a second part, the results of reservoir and environment monitoring during the mobile ORC test are presented and discussed.

Several MEET deliverables are related to this one:

- D3.4: Characterization of scaling (Public)
- D3.8: Fiber optic behaviour in very saline conditions (Confidential)
- D3.9: Hydro-thermal model using VSP analysis and colder reinjection tests (Public)
- D6.5: Summary of additional heat production capacities at the Soultz sous Forêts site (Public)
- D6.9: Performance results analysis report from the 3 first demo-sites (Public)

1.2 BRIEF DESCRIPTION OF THE STATE OF THE ART AND THE INNOVATION BREAKTHROUGHS

The Soultz-sous-Forêts EGS power plant is one of the most famous in the world due to the intensive research performed there over 30 years. Based on the knowledge and experience gained on this site, new EGS plants were built in the Upper Rhine Graben in the last decades (Vidal et Genter, 2018). These plants produce very saline geothermal fluids (Total Dissolved Solids (TDS) of 100 g/L) at 150-170°C with similar physico-chemical characteristics (Sanjuan et al., 2016 and Bosia, 2021), and reinject them at about 70°C with a current limit set at 60°C.
This highly saline fluid induces scaling formation in the surface facilities and in the wells, triggered by the changes in pressure and temperature in the plant (Scheiber et al., 2012, Mouchot et al., 2018). Even if the trigging factors for scaling precipitation in Upper Rhine Graben have been discussed, only a few geochemical modeling were performed to attempt to numerically reproduced this phenomenon (Kirknel et al, 2019).

In MEET project, the feasibility of reinjecting at lower temperature, down to 40°C is investigated.
On-site tests have been performed to reduce reinjection temperature down to 40°C. A first test on 10% of the flow rate to investigate scaling phenomenon in a small heat exchanger and a second test where all the flow rate was derived into a small mobile ORC (called “Mini-ORC”) provided by ENOGIA to produce electricity a low temperature.

Detailed characterization of scaling has been performed at this very low temperature for the first time (MEET Deliverable D3.5 and Ledesert et al, 2021). In the current deliverable, a detailed geochemical modelling of scale precipitation at different temperature steps (from reservoir temperature down to 40°C) is presented. It helps deciphering thermodynamic effect for kinetic effects inducing or preventing certain scale precipitation. It also highlights the lack of kinetic data for specific species in operational condition.

In parallel with the mini-ORC test, the monitoring network of Soultz power plant has been enhanced in order to better identify any impact of colder reinjection on the reservoir and the environment. Among the sensor deployed, a fiber optic has been installed in an observation well. Many attempts have been performed these last years to use optic fiber to record temperature and acoustic measurements in deep wells (Hurtig et al., 1997, Mateeva et al., 2014) and this tool is progressively implemented in the panel of monitoring tools for the geothermal industry. In MEET, in addition to temperature and acoustic measurements, innovative treatment of the optic signal has been developed to derive a distributed pressure profile.

1.3 CORRECTIVE ACTION (IF RELEVANT)

This deliverable was initially due for end of April 2021. However, due to COVID-19 situation, Mobile ORC delays in Work-Package 6 and Soultz plant shut-down between September 2020 and February 2021, many relevant data to produce this deliverable were delayed. It is finally submitted by end of September 2021.

1.4 IPR ISSUES (IF RELEVANT)

N/A

2 DELIVERABLE REPORT

2.1 SOULTZ-SOUS-FORETS SITE PRESENTATION

The Soultz-sous-Forêts power plant is located at around 50 km north of Strasbourg (France) in the Upper Rhine Graben (URG) which is known as a great potential for the exploitation of geothermal energy at high temperature. Indeed, the geothermal gradient in continental crust is about 30°C/km, but around the Soultz sous-Forêts (SsF) power plant, it can reach up to 100°C/km in the sedimentary layers (Figure 1).

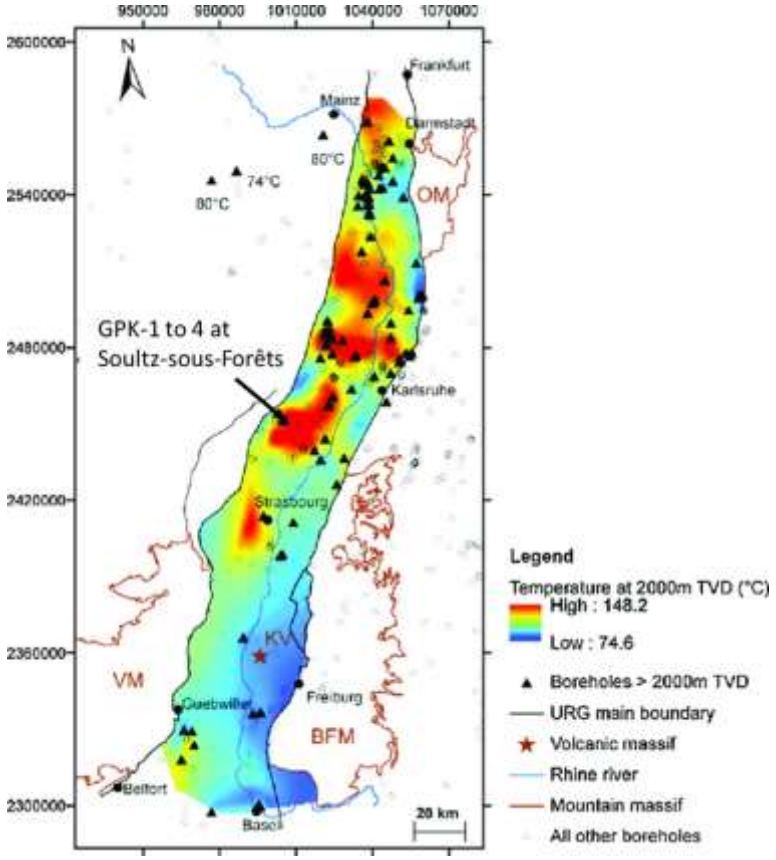

Figure 1: Temperature distribution at 2000 m TVD in the Upper Rhine Graben (modified after Baillieux et al., 2013 based on Agemar et al., 2012 and Pribnow and Schellschmidt, 2000).

The geothermal project began in 1984 and first drilling began in 1987 (Gerard et al., 2006). The initial goal was to use the heat in the deep crystalline rocks to produce electricity by fracturing the granite to create an artificial reservoir as an HDR (Hot Dry Rock) project. For this, a first phase of drilling and observation was done until 2007 to study the crystalline rock and the feasibility of future operations. In total 9 wells have been drilled or deepened in this period (Figure 2):

- GPK-1, the first well is now plugged
- GPK-2, GPK-3, GPK-4 are currently used in the plant exploitation
- EPS-1, 4550, 4616, 4601, OPS4 are available to install sensors for observation purpose.

Hydraulic and chemical stimulations were done to increase the permeability and the connections between the reservoir and the wells. It has been shown that permeability creation or enhancement is largely limited to weak natural fractures, which are elements of hydrothermally altered, cataclastic shear zones that intersect the borehole (Evans et al, 2005). A geothermal fluid is naturally circulating through these fractures which is a 100 g/l NaCl type brine (Sanjuan et al., 2016). The concept thus gradually switched from HDR to Enhanced Geothermal System (EGS).

The site gradually shifted from research to industrial facility. The initial power plant from 2008 was refurbished in 2015 and the industrial electricity production began in June 2016. The owner of the Soultz plant is the EEIG Heat Mining (or “GEIE Exploitation Minière de la Chaleur”), while the geothermal plant operation and maintenance is performed by ES-Géothermie.
Currently, the geothermal site exploits around 30 L/s of geothermal fluid. The brine is produced at 150°C from the production well GPK-2 and conveyed after filtration to three heat exchangers supplying heat to a 1.7 MW ORC (Organic Rankine Cycle) unit. This electricity production unit is the only heat user of this geothermal plant, and uses the ambient air as a heat sink, through an Air-Cooled Condenser. The ambient air temperature variations throughout the day and the year impact the geothermal brine reinjection temperature, ranging from 60°C to 80°C. The geothermal brine is reinjected into two different wells, GPK-3 and GPK-4.

Figure 2: Location and view of the Soultz-sous-Forêts site (source: ES).

2.2 COLDER REINJECTION TESTS OVERVIEW

The objective of Work Package 3 of MEET project is to assess the feasibility to lower the reinjection temperature on EGS plant in the Upper Rhine Graben from 70°C down to 40°C. This colder reinjection would allow to valorise more energy with the same facilities. Two colder reinjection tests were performed on the SsF site: one with a small heat exchanger to study scaling precipitation down to 40°C and assess the behaviour of different metallurgies and the other one to test the production of electricity at these low temperatures with a small mobile ORC unit (called Mini-ORC).

2.2.1 Small heat exchanger test

From February to April 2019, 10% of the flow coming from the heat exchangers of SsF plant has been diverted into a prototype heat exchanger before being sent back in the injection well. This prototype was designed with four passes of 8 to 9 tubes, using 6 different metallurgies: 1.4539 (904L), 1.4547 (254 SMO), 1.4462 (DX 2205), 1.4410 (SDX 2507), 2.4858 (Alloy 825) and 3.7035 (Ti Gr.2). Figure 3 presents the drawing of the prototype heat exchanger as well as its end plate and shows how the different alloys for the tubes were implemented.

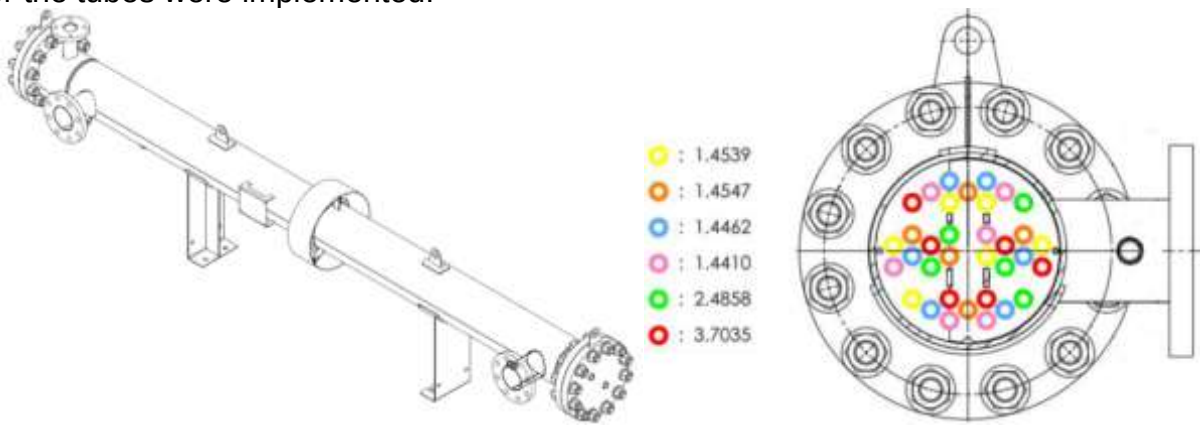

Figure 3: Drawings of the prototype heat exchanger (left) and of the end plate design showing the metallurgies used (right).

After 3 months of operation, the heat exchanger has been dismantled. Scaling and corrosion analyses have been performed to assess the behaviour of the fluid in a temperature range from 70 to 40°C regarding different metallurgies tested. Detailed results of these investigation have been reported in MEET Deliverable D3.5 and published in Ledesert et al., 2021.

2.2.2 Mini-ORC test

2.2.2.1 General presentation

The Mini-ORC has been designed and manufactured by ENOGIA in the framework of work package 6 of MEET project. It was delivered on SsF plant in August 2020 but could only start beginning of March 2021. Indeed, a production pump failure induced a stop of SsF plant operation between September 2020 and end of February 2021.
The Mini-ORC was fully operating from March 13th until June 15th 2021 (see Figure 4), for a total operation time of 3 months.

Figure 4: Mini-ORC installed on the Soultz-sous-Forêts power plant.

Preliminary results indicates that the Mini-ORC delivered a power production between 10 and 20 kW, for a turbine designed for 40 kW max. Production is highly dependent on ambient temperature, the lower the ambient temperature the better the production (Figure 5).

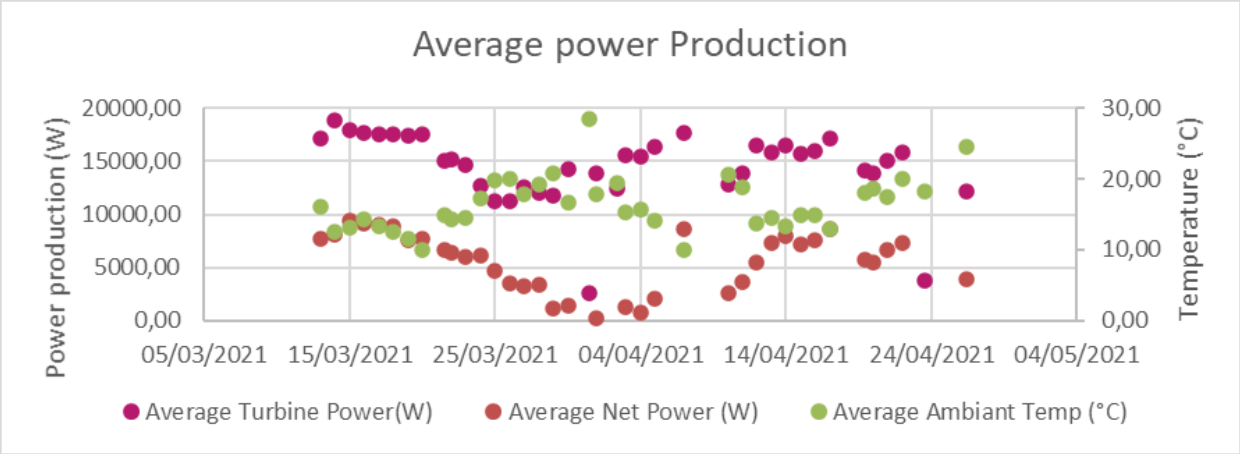

Figure 5: Plot of the average power production, and ambient temperature on the Soultz-sous- Forêts demonstration site (these preliminary results do not show the entire testing sequence) (modified from Deliverable 6.9).

2.2.2.2 Monitoring network

Early 2020, several surface and downhole monitoring instruments were installed onsite or in the direct vicinity of the Soultz-sous-Forêts geothermal plant. The main goal was to monitor the effects on the reservoir of the reinjection of a colder geothermal brine induced by the installation of the ENOGIA Mini-ORC onsite. The main expected effects caused by this colder brine reinjection were a change in the hydrological parameters of the reservoir such as a change in pressure and temperature and a change in the rate of induced seismicity. Hence, the seismic monitoring network was densified, a series of piezometers

were installed in 3 peripheral observation wells and as well as a fiber optic in the well EPS-1, which is the closest to the area of reinjection.

Seismic monitoring network:
Since 2012, the micro-seismicity induced by the Soultz-sous-Forêts geothermal power plant has been monitored by a network of 7 permanent surface seismological stations (see Figure 8).
It is composed of:

- 6 short-period seismological sensors (1 Hz, L4C), with 3 components (see Figure 6)
- 1 short-period seismological sensors (1 Hz, L4C), with 1 component,
- 1 large-band seismological sensor (120 s) with 3 components installed with an accelerometer (4g +/- 0.25 g), 3 components

Figure 6: (Left) Seismometer L-4-3D (1 Hz), (Right) Centaur CTR-3S datalogger.

The signals from the stations are digitized by Centaur CTR3-6S or CTR-3S directly in miniSEED format with a sampling step of 200 Hz. The signals are then transmitted by 3G to the ESG server where they are automatically processed, allowing to generate an alarm by email, SMS and vocal message in case of potentially felt induced earthquake. The Rittershoffen seismic network, dedicated to the seismic monitoring of the Rittershoffen geothermal plant was also used in this project (Figure 8).

In the framework of this study 3 low-cost raspberry shake instruments (Figure 7) were installed early 2020 to densify the existing seismic monitoring network. The goal was double: first to test this new technology and second to increase the sensitivity of the network, allowing to detect lower magnitude events.

Figure 7: Rasperry shake instrument

The Figure 8 shows the location of the Soultz and Rittershoffen networks and the location of the raspberry shake instruments installed in the framework of this project.

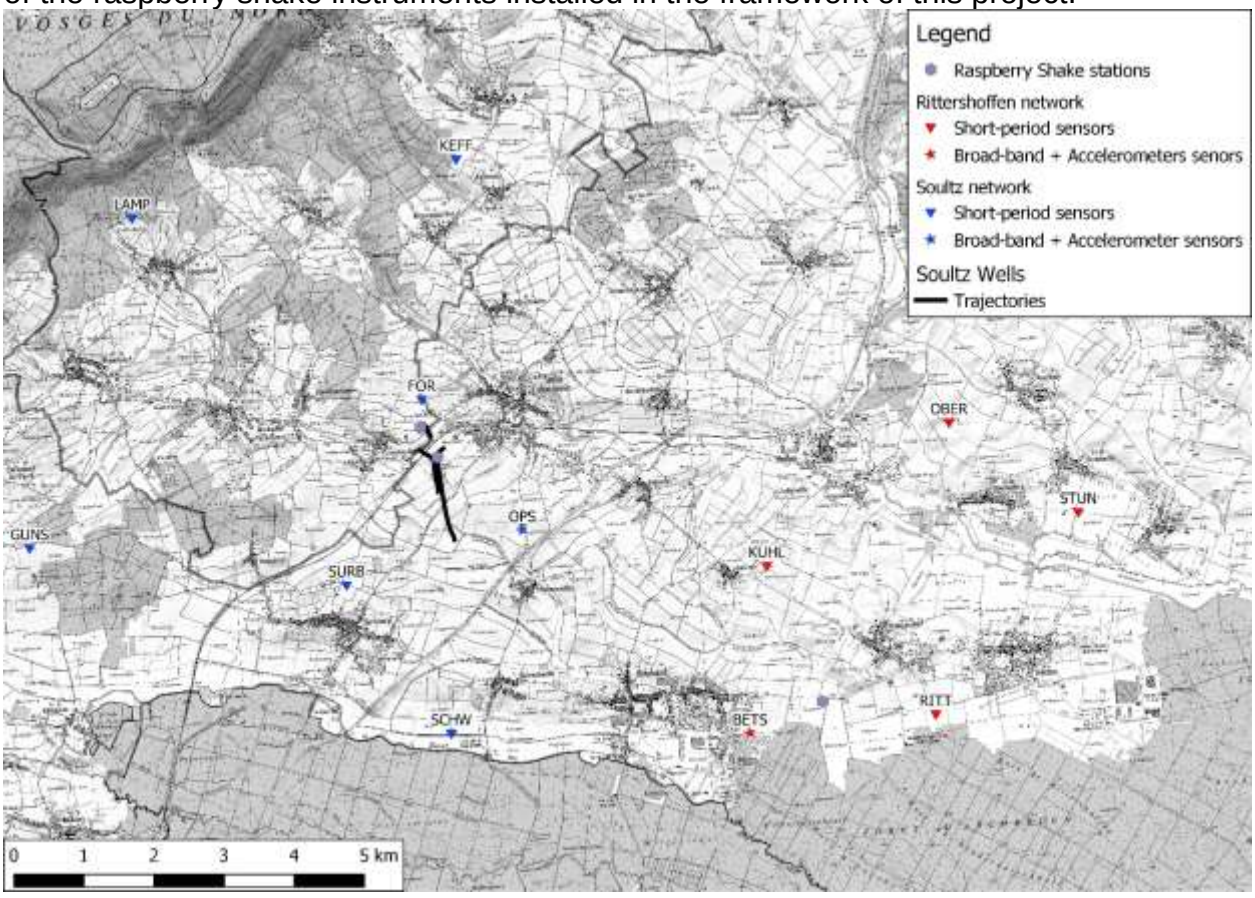

Figure 8: Seismic monitoring network from Soultz and Rittershoffen and the 3 raspberry shake instruments installed in the framework of this project.

Piezometers network:

In the framework of this project, 3 piezometers were installed in peripherical observation wells in the close vicinity of the geothermal plant of Soultz-sous-Forêts. The main goal of this installation was to observe the potential changes in terms of temperature and

pressure into the reservoir due to the colder reinjection. Three OTT ECOLOG 800 piezometers (see Figure 9) were installed at the end of 2019 in the observation wells called 4601, 4616 and 4550, located westwards and northwards of the plant (see Figure 10). The piezometers are installed at a depth of 100 m, and can record the temperature, the conductivity and the water level. Data are transmitted via a 2G/3G connexion and are directly stored on a ESG server, visible in real time. The Figure 11 gives a picture of an example of an installation.

Figure 9: OTT ECOLOG 800 piezometers.

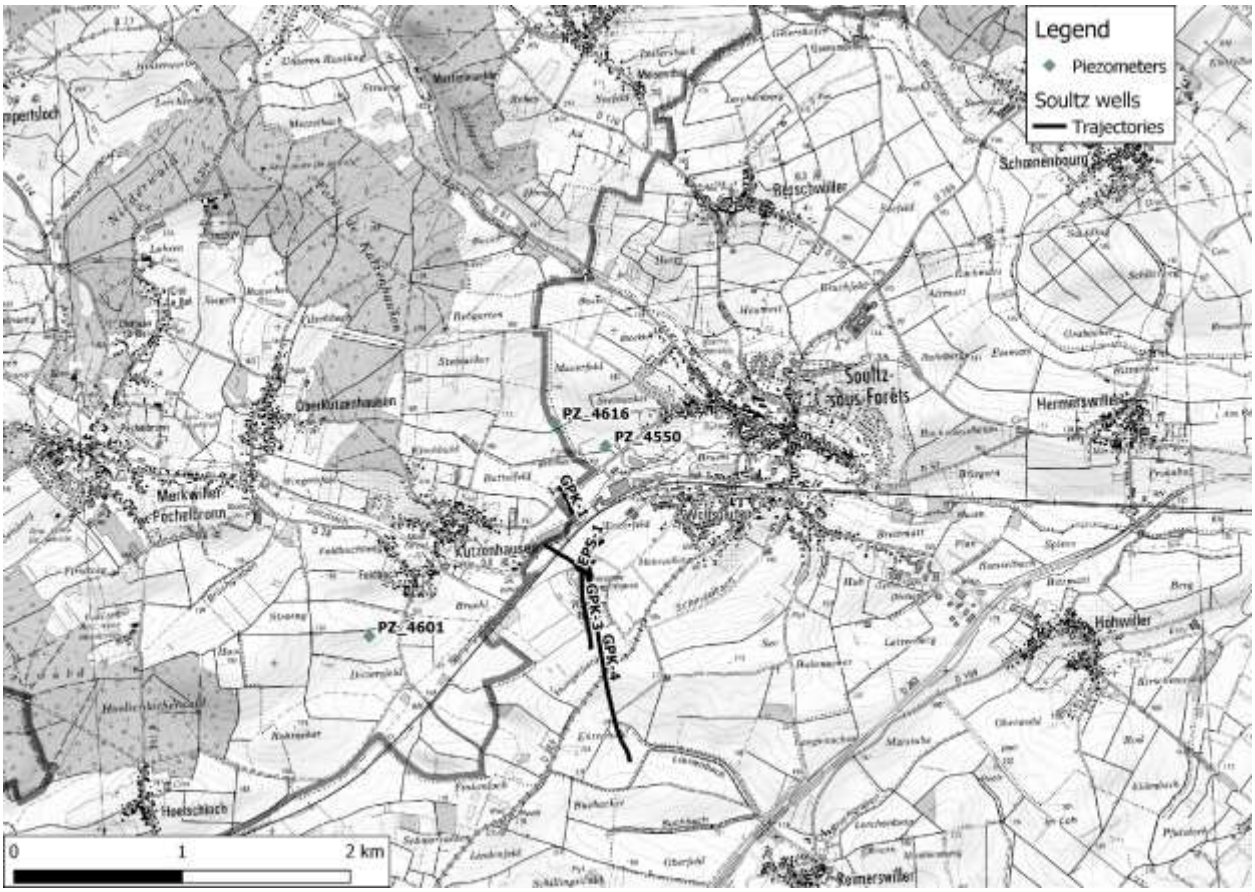

Figure 10: Location of the piezometers network compared to the Soultz-sous-Forêts wells.

Figure 11: Example of an installation on the 4616 well.

Fibre optic installation:

In the framework of MEET, in order to monitor the plant, FEBUS Optics is in charge for the deployment and exploitation of a fibre optic cable in the observation well EPS-1 located in Soltz-sous-Forêts (Figure 10). The deployment of this cable, in end of July 2021, has been coordinated by ES-Géothermie (Figure 12).

Figure 12: Second operation of fibre optic cable deployment in the observation well of the Soultz-sous-Forêts geothermal plant.

The installation of this fibre optic cable in EPS-1 enabled the monitoring of various physical parameters using different Distributed Fibre Optic Sensing technologies. Indeed, Distributed Fibre optic Sensing is an innovative technology allowing to turn a fibre optic

cable into hundreds to thousands of sensors. This technique relies on the use of the backscattered light of a LASER pulse sent along the fibre. Depending on the backscattering mechanism, different information can be retrieved about the fibre neighbourhood (Hartog, 2017):

- Raman scattering is used for the study of the temperature variations along the fibre. The system associated with this process is called DTS or Distributed Temperature Sensing.
- Brillouin scattering enables the analysis of temperature and strain changes. This technique is depending on the environmental changes at the fibre vicinity and is named Distributed Strain and Temperature Sensing (DSTS).
- The focus on the Rayleigh scattering is associated with DAS (Distributed Acoustic Sensing). The phase-sensitive DAS systems rely on the use of the relation between the phase difference of the backscattered light between two portions of the fibre and the dynamic strain the fibre is subject to. Thus, this kind of interrogator will detect any acoustic wave with a sufficient coupling to excite the cable.

Since the installation of the fibre optic cable in EPS-1, several acquisition campaigns have been achieved using the three monitoring devices described above.

2.3 GEOCHEMICAL IMPACT ON THE FLUID

2.3.1 Scaling observations in the heat exchangers

Results of scaling observation in the small heat-exchanger have been deeply reported in MEET Deliverable D3.5 and published in Ledesert et al., 2021.
The main conclusion is that scales are very homogeneous whatever the metallurgy and the temperature, from a global point of view. They are Arsenic-Antimony-rich Lead sulphides of galena type. Some halite (NaCl) has also been found. It is interpreted as late deposits taking place during operational maintenance and/or shutdown.
Detailed chemical analyses performed by ICP-MS show a lowering of Pb and Sb contents while As increases, from 60°C to 50°C in all the samples. Small amounts of Si were also quantified, as well as Fe and Cu in the sulphide matrix.

SEM observations highlighted two different structures, and likely growth episodes, of scales: a smooth, compact and thin structure attached to the metal, and a thicker (in general) and younger porous layer. A few samples do not show this structure as they occur naturally as a powder (in entrance and water boxes) or since they lost their structure during sampling due to necessary scratching of tubes on which they adhered strongly (2205 and $TiGr_2$).

Figure 13. Left: PbS scales deposited in tubes from the test heat exchanger, Right: Microscopic photo of (Pb,As,Sb)S scale found at SsF plant (Ledésert et al., 2021).

In addition to these observations in the framework of MEET project, scales in the range between 150°C and 65°C have been sampled in June 2018 before cleaning operation in the ORC evaporator and preheaters after nearly 1 year of operation. Chemical composition of these scales has been determined using ICP MS method. At production temperature, the amount of scales is very low and they are mostly composed of carbonates. When the temperature decreases inside the heat exchangers, the global amount of scales increases and metal sulphides becomes dominant at temperature lower than 100°C (see Table 1). It is important to note that sulphate inhibitor is used in the SsF plant since 2016, which impacts both scale composition in SsF heat exchangers and MEET test heat exchanger. Without this inhibitor, scales known at low temperature are mostly composed of Barium sulphate with a minor amount of sulphides (Haas-Nüesch et al., 2018).

Table 1: Mass composition of scales formed in the heat exchangers at the geothermal plant and in the test heat exchangers in percentage (from Kunan et al., 2021).

Temperature [°C]	S	Pb	Sr	Ba	Sb	As	Fe	Si	Cu	Total	Exchanger
150	2.9%	2.0%	2.9%	0.9%	0.1%	0.5%	1.7%	3.8%	0.4%	15.3%	ORC Inlet Evaporator
120	10.4%	13.0%	0.7%	0.6%	1.1%	4.2%	4.0%	6.2%	15.1%	55.3%	ORC Outlet Evaporator
120	11.8%	26.5%	0.7%	1.9%	3.3%	6.6%	7.5%	8.0%	16.6%	82.9%	ORC Inlet Preheater
90	11.2%	36.1%	0.9%	3.6%	3.1%	5.2%	8.0%	16.9%	5.1%	90.1%	ORC Preheater
65	13.1%	46.3%	0.5%	2.2%	6.3%	7.3%	4.6%	8.4%	4.5%	93.2%	ORC Outlet Preheater
60	13.1%	74.6%	0.0%	0.0%	6.4%	3.2%	0.1%	1.4%	0.4%	99.2%	MEET Test HEX
50	14.4%	66.5%	0.0%	0.0%	11.4%	4.3%	0.6%	1.0%	0.4%	98.6%	MEET Test HEX
40	16.7%	64.2%	0.0%	0.0%	10.9%	4.5%	0.5%	1.6%	0.4%	98.8%	MEET Test HEX

2.3.2 Geochemical modeling

Detailed geochemical modeling conducted in the framework of MEET WP3 is presented in Kunan et al., 2021 (submitted to journal Geosciences) and available in Appendix 1.

The modelling of the geochemical fluids has been done through the software, PhreeqC which is designed to perform numerous aqueous geochemical calculations. It implements several types of aqueous models depending on the database used. An intensive work has been conducted on geochemical databases to identify which one would be best suited regarding elements and minerals observed in the fluid and in the scales. Overall,

the Thermoddem database was selected for the modelling of the formation of scales in the geothermal fluids and Pitzer database is recommended for modelling of the dissolved gas in the fluid. It has been ensured that these databases are appropriate in the temperature range of observation as well as valid in regards of ionic strength of the fluid.

Four modeling have been performed: 2 thermodynamic modeling and 2 kinetic modeling. The first thermodynamic modeling was run to identify possible mineral precipitation and without elemental restriction. It showed that principal mineral to precipitate should be silicates with a minor amount of barium surface at all temperature. However, this composition is far from the observations made. It is suspected that silicate precipitation takes too long to be observed in scale deposited in the heat exchangers. Additionally, sulfates are currently inhibited by the use of dedicated treatment.
The second thermodynamic modeling is performed without sulfate and silicates to better reproduce observed scales composition. For each step of temperature, the modelling results show that sulphur and iron are the major elements with concentrations of 45% and 53%. On the other hand, the total amount of the other elements represents less than 3% of the total. Copper is only found at 40°C and in extremely small quantities. Antimony and lead are also found in small quantities (less than 1.5%) at any given step of temperature.

The results given out by the calculation of the thermodynamic model gives insight on the precipitation of the minerals at thermodynamic equilibrium which may not necessarily be respected in the plant operation conditions.
For the initial kinetic model following minerals are considered: amorphous silica (SiO_2), quartz(alpha)(SiO_2), galena (PbS), orpiment (As_2S_3), pyrite (FeS_2), and stibnite (Sb_2S_3).
This kinetic model showed improvements in the results when compared to the first thermodynamic model. The kinetic model has significantly reduced the Si and O contents for the temperatures between 65°C and 150°C. This confirms that the kinetic effect controls the absence of silicates in the SsF scales. However, for this range of temperature, sulphur (S) and iron (Fe) have the highest concentrations with the highest percentage being 52.2% and 45.1% respectively. Regardless, the concentration of each element for the kinetic model 1 does not reflect the actual concentration found in the SsF plant analyses.

The discrepancies can be explained by the conditions of the modelled scales being outside the domain of validity for temperature and pH of the kinetic information used. Therefore, to better simulate the scale formation at the SsF geothermal plant, a modified version of the initial kinetic model was created. In this second model, the kinetic information of the minerals was modified to reflect closely to the observation done on SsF plant. All things considered, this model allows a rough prediction on the scale formation when operating the plant with sulphate scales inhibitors at the SsF geothermal plant as there is only a small deviation between simulated results and the actual case. The model becomes less accurate at higher temperatures such as at 150°C because of the lack of antimony and arsenic at this temperature.

2.3.3 Discussion

For the thermodynamic modelling, this method is done over a great amount of time which is impractical for predicting the formation of scales in an actual case. The saturation index obtained from thermodynamic modelling however is a good indication on which mineral can precipitate in function of the temperature.

For the kinetic modelling, specific kinetic information such as the rates equation and the kinetic constant for the precipitation of the mineral are lacking for the desired range of temperature. Nevertheless, the modelling shows that silicate precipitation is strongly controlled by kinetic. Additionally, this method allows a more accurate prediction for the formation of scales with the caveat of having the proper kinetic information.

The results obtained in this study open new perspectives on the issue of lack of kinetic information. Bibliographic research was concluded to be insufficient and future laboratory studies, tests and analyses should be done on the precipitation of minerals at the working conditions of SsF geothermal plant.
The scale inhibition should also be analysed and studied to be integrated into the current model. Laboratory studies should be done to identify any additional reactions that contribute to the formation of scales. The kinetic information obtained from laboratory studies on additional reactions should also be integrated into the current model. With precise kinetic information on the precipitation of the minerals and considering other possible reactions, a more accurate prediction model can be created for future uses.

2.4 IMPACT ON THE RESERVOIR

2.4.1 Observation from the monitoring network

2.4.1.1 Temperature observations

Figure 14, Figure 15 and Figure 16 show the temperatures measured by the 3 piezometers between 12.2019 and 09.2021. The temperature is very constant over the whole period of recording at 19.6°C at PZ_4601, 22.9°C at PZ_4550 and 20.6°C at PZ_4616. Some very small drops (0.05°C) of the temperature are visible on the temperature of PZ_4550, but these drops are not correlated to the period of injection of colder brine since they occur before.

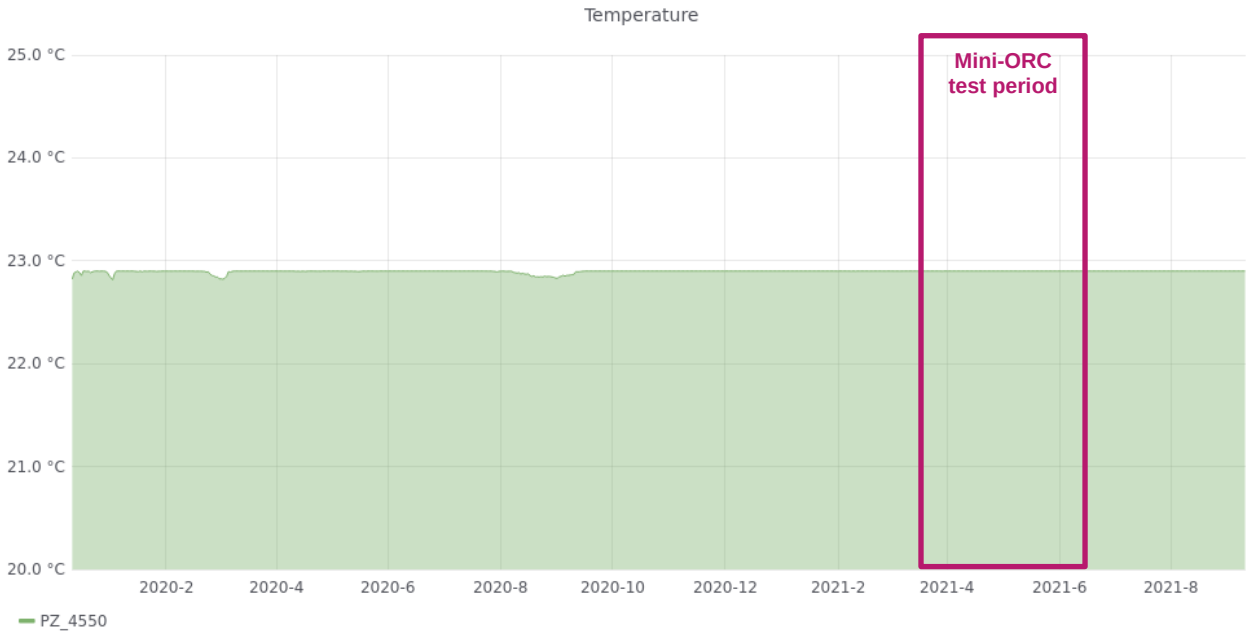

Figure 14: Temperature measured by the piezometer PZ_4550 between 12.2019 and 09.2021.

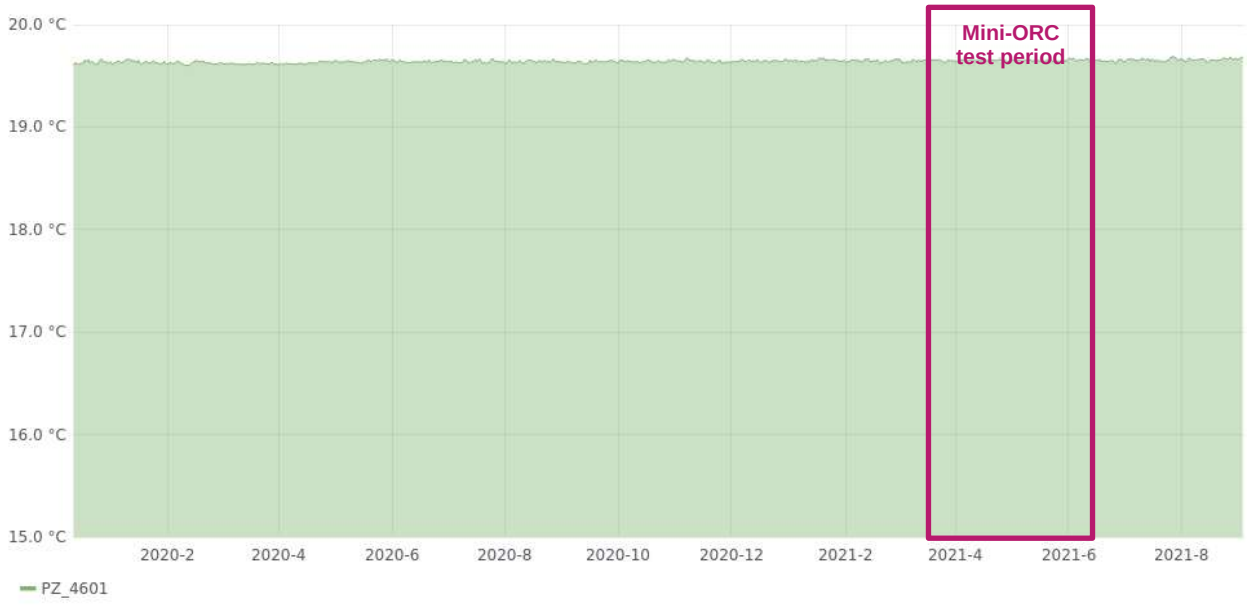

Figure 15: Temperature measured by the piezometer PZ_4601 between 12.2019 and 09.2021.

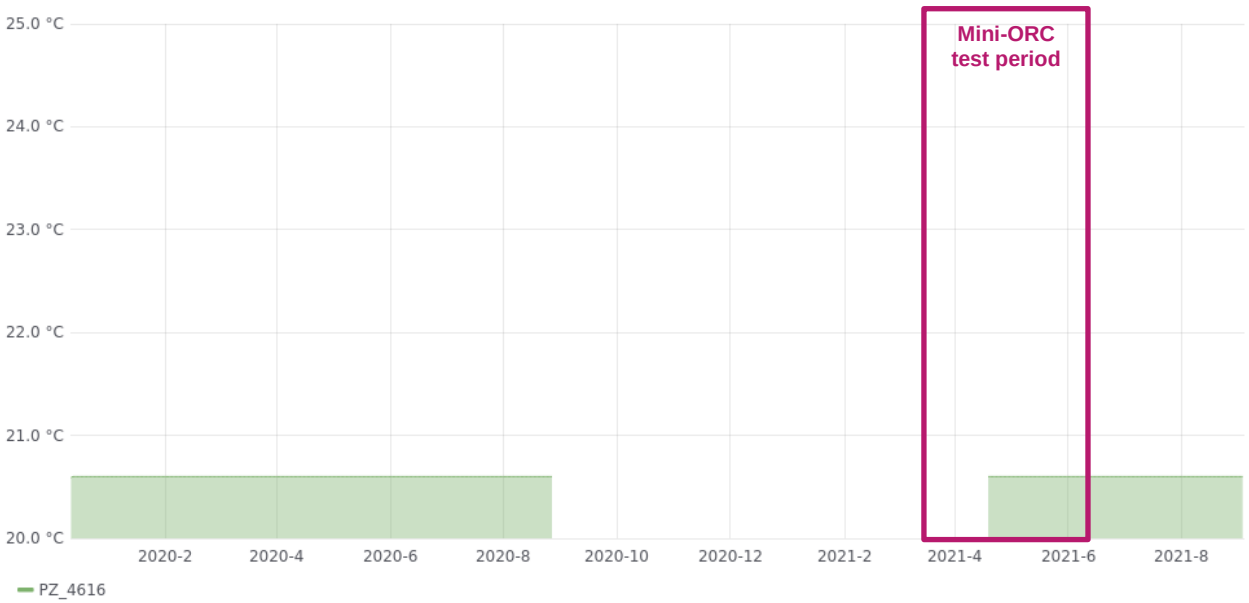

Figure 16: Temperature measured by the piezometer PZ_4616 between 12.2019 and 09.2021.

The Ecolog sensor of PZ-4616 was damaged in August 2020 and had to be repaired. It resumed operation in April 2021.

Distributed Fibre Optic Sensing results:

Acquisitions using Distributed Temperature Sensing (DTS) have been achieved along fibre optic cable deployed in EPS-1 observation well located in Soultz-sous-Forêts geothermal plant in July 2020 (orange curve in Figure 17). They appear in very good correlation with a log previously achieved in EPS-1 well and provided by ES Géothermie (green curve in Figure 17). Moreover, the observed gradient corresponds to the one expected in this area of the Upper Rhine Graben: a high gradient reaching 100°C/km over the first kilometre and lowering to around 30°C/km after this step.
Moreover, Distributed Strain and Temperature Sensing (DSTS) data, acquired along the same cable, show a lot of similarities with DTS acquisition with a same shape in the curve and changes in slopes. However, we observe a deviation in temperature values, amplifying with depth, between those two acquisitions. DSTS, as explained in section 2.2.2.2, consists in a coupled measure of temperature and strain along the fibre cable. This observed deviation can then be explained by the strain contribution.

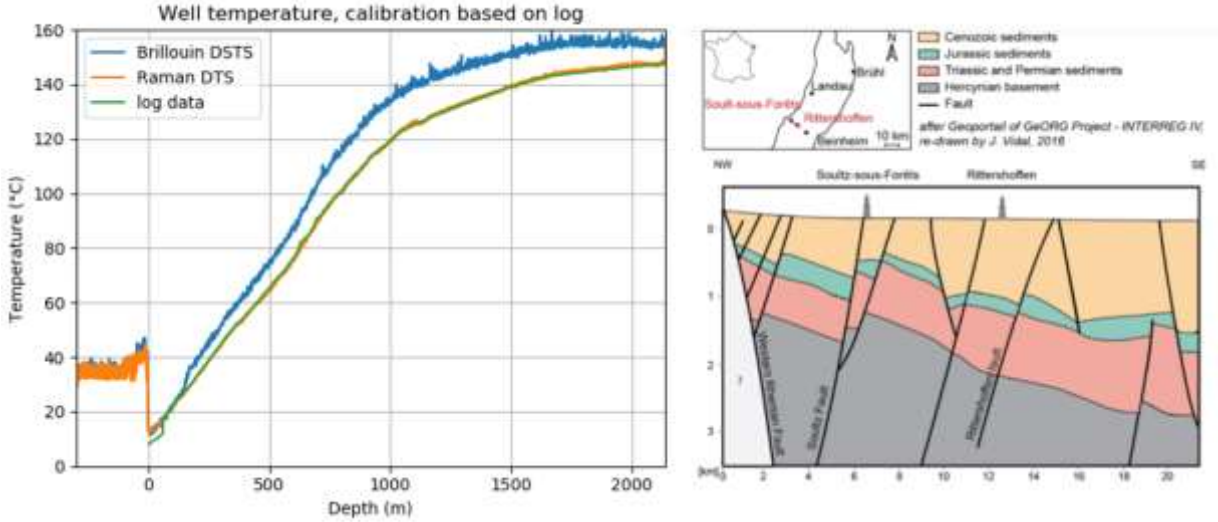

Figure 17 Left: Temperature measurements achieved with DTS (orange) and DSTS (blue) right after fibre optic cable deployment. Those results are compared to log previously achieved with classic techniques in EPS-1 (green). Right: Geological cross-section through Soultz-sous-Forêts and Rittershoffen geothermal plants [Vidal and Genter, 2018].

2.4.1.2 Pressure observations

The Figure 18, Figure 19 and Figure 20 show the altitude of the water level recorded by the 3 piezometers between 12.2019 and 09.2021.

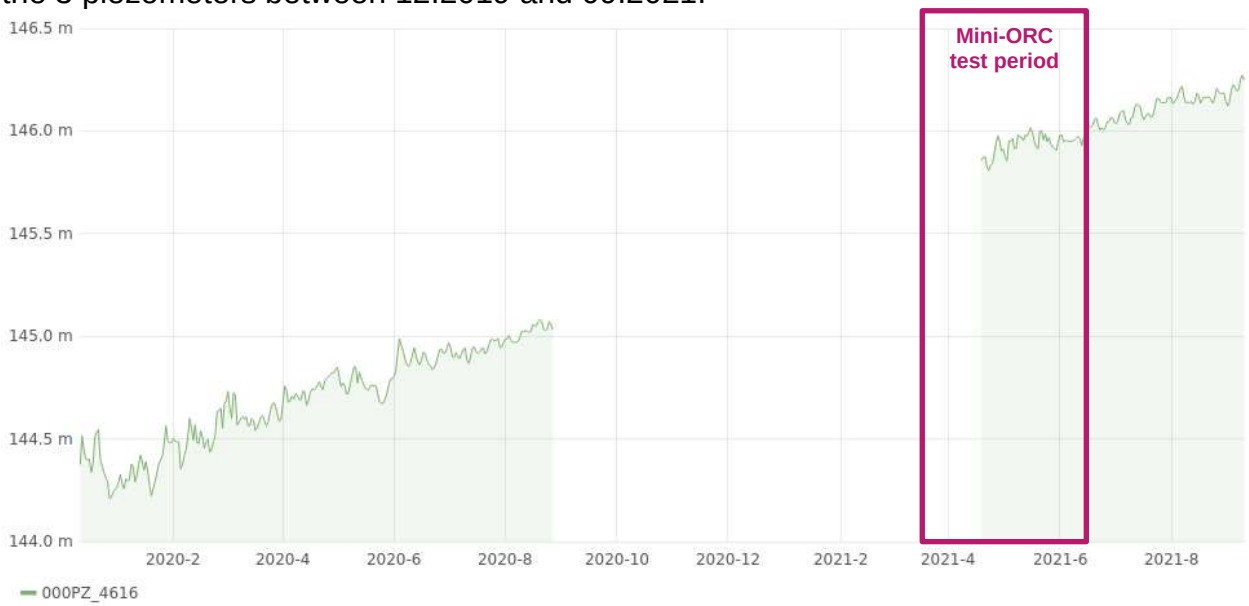

Figure 18: Altitude of the water level from the piezometer PZ_4616 between 12.2019 and 09.2021.

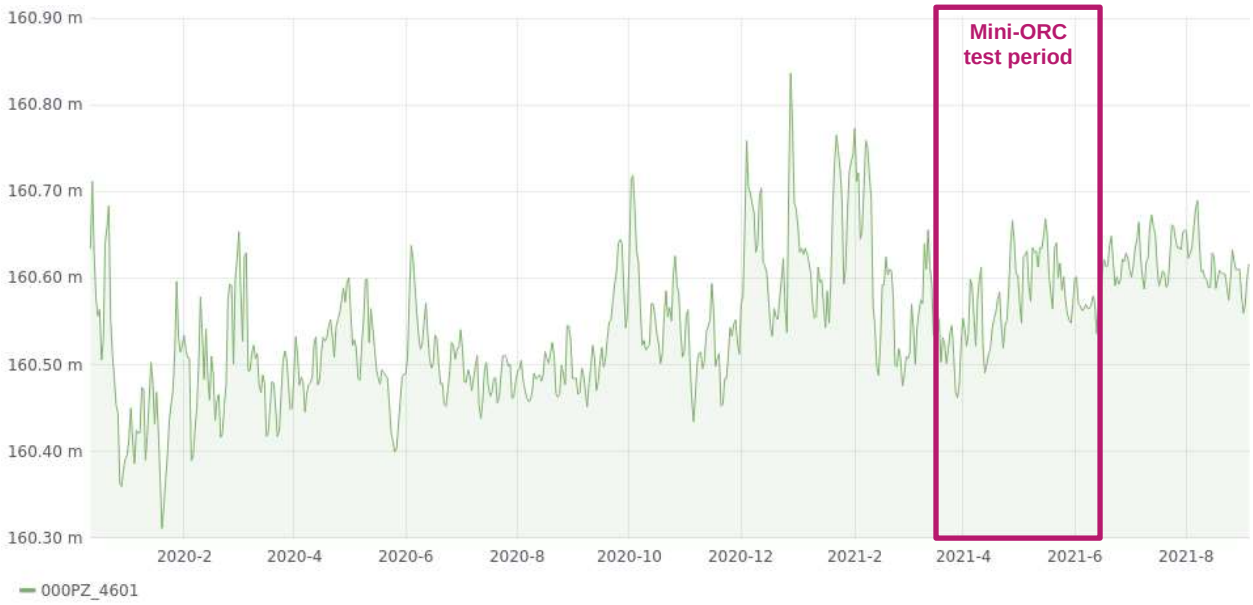

Figure 19: Altitude of the water level from the piezometer PZ_4601 between 12.2019 and 09.2021.

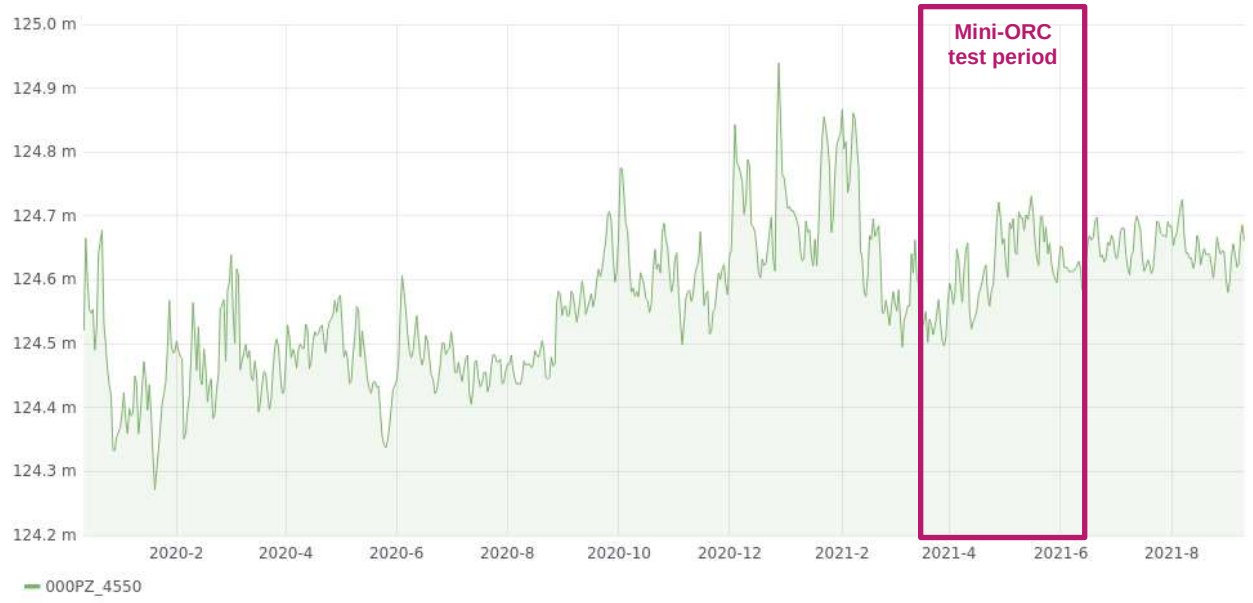

Figure 20: Altitude of the water level from the piezometer PZ_4550 between 12.2019 and 09.2021.

The altitude of the water level recorded by the piezometers stayed quite constant for PZ_4550 and PZ_4601 during the time period of the project. However, the water level measured by PZ_4616 showed a constant increase during the time period of the project. This trend visible during the whole period seems to be more in relation with the dilution of the salted plug injected to kill the well rather than with the Mini-ORC test. Many small variations of the altitude of the water level, which are similar between wells, are also visible since the beginning of the records. For example, the altitude of the water lever is higher in the wintertime of the year 2020 and there is a correlation of these small variations on the three piezometers over the whole recording period. These variations are

mostly related to variation of atmospheric pressure and tidal effect (Baujard et al., 2017). No clear signal in the water level can be attributed to the injection of the colder water.

Distributed Fibre Optic Sensing results:

Results of the acquisition using Distributed Strain and Temperature Sensing along the fibre optic cable deployed in EPS-1 observation well are presented in Figure 21. As mentioned above, we observe a deviation between the DSTS and the DTS curves. This deviation is explained by the dual acquisition of strain and temperature when using the DSTS.
We conducted a DTST acquisition 7 months after the fibre optic cable deployment in EPS-1 well. When achieving this acquisition, we emphasized the presence of a progressive optical loss of around 5 dB from a depth of around 800 m in EPS-1 well. This attenuation could be related to a water ingress on the wireline cable compressing the fibre proportionally to its depth. Thus, this event could conduct, with the use of DSTS, to an estimation of the pressure gradient in EPS-1. The combined use of DTS, providing pure temperature profile, and DSTS can then conduct to the estimation of a pressure profile in EPS-1 well (Figure 15).

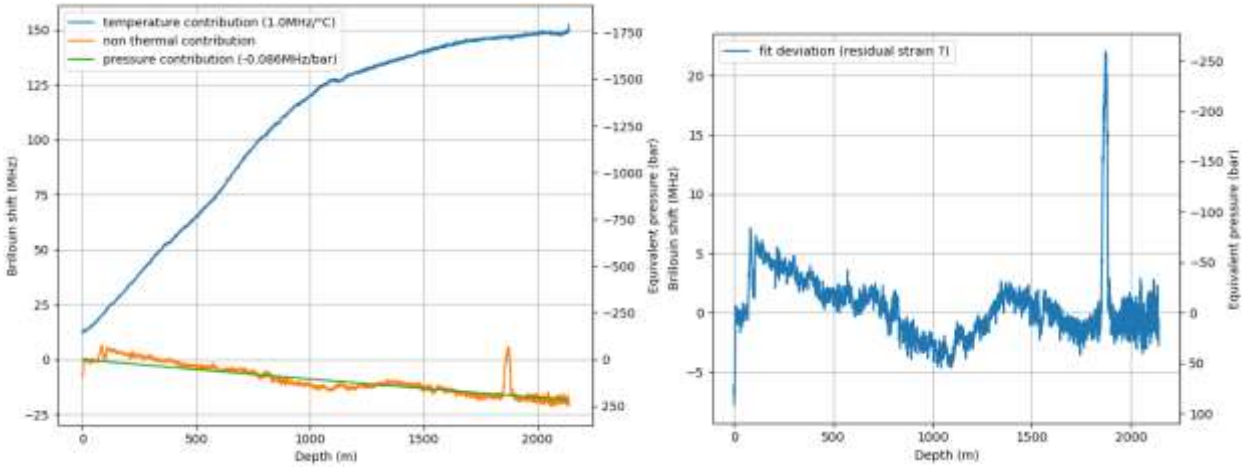

Figure 21: Left: Temperature (blue) and non-thermal contributions (orange) profile extracted from Distributed Strain and Temperature Sensing acquisition (Figure 11). Non-thermal contributions are compared to the theoretical pressure gradient of the area (green). Right: residual strain related to the position and/or the tension in the fibre optic cable deployed in EPS-1 well.

The non-thermal contribution curve (orange) observed in Figure 21 is compared to a theoretical pressure gradient (green curve) estimated from the density of the water in EPS-1 well:

$$\rho = -0.0025\,T^2(z) - 0.2758T(z) + 1083.7$$

$$P(z) = \int (-0.0025\,T^2(z) - 0.2758T(z) + 1083.7)g\,dz$$

With ρ the density, T the temperature, g the gravity acceleration, z the depth from the water level and P the pressure.
We observe that the results of this comparison are in good correlation involving a good ability, in these conditions, for the DSTS to measure pressure. Additionally, it is highly probable that the initial slope (from 200 to 1.000 m) which is higher than the one anticipated with geothermal brine reflects a higher density from a brine plug used to kill the well, whereas the bottom of the well (1.800 – 2.200 m) reflects a density closer to the geothermal brine. This non-thermal contribution of Brillouin signal is thus a good indicator of pressure all along the well. However, it cannot be excluded that it also contains signal coming from static stretches along the fibre cable due to its position, with tensions or torsions, in the well.

Moreover, DSTS profiles have been achieved before and after the installation of the ORC in the Soultz-sous-Forêts geothermal plant at the end of February 2021 and in May 2021 (respectively 7 and 10 months after the fibre optic cable deployment). Figure 22 presents the results of this acquisition.
We can observe a peak at 1.8 km depth corresponding to a strain event. It may be related to a torsion of the fibre optic cable at this position. We observe an amplification of the phenomenon with time with an increase in amplitude and width of the event. Special attention will be paid in this area after cable recovery. This event is now closely monitored to avoid any break along the cable.

Additionally, it seems that the temperature increased from a few degrees between February and May 2021 below 1.500 m, which corresponds to reservoir depth. It is not clear whether this corresponds to a real temperature shift or to an artefact due to tension and torsion on the cable.

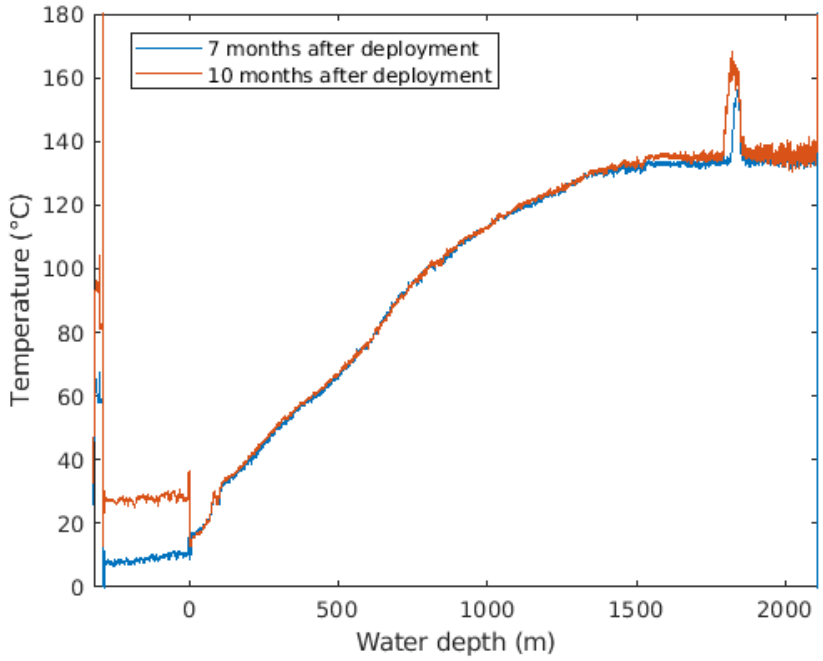

Figure 22: Combined temperature and strain profile extracted from DSTS acquisition 7 months after deployment, in February 2021 (blue) and 10 months after deployment, in May 2021 (red).

2.4.1.3 Microseismicity

Between 01-01-2020 and 01-09-2021, 108 significant events were detected, including 54 linked to geothermal operations in Soultz-sous-Forêts. Figure 23 shows the microseismic activity observed during this period (number of events detected per day). During the Mini-ORC test, no induced event was recorded, only natural ones.

Thresholds on magnitude and Peak Ground Velocities (PGV) are in place at ESG to be able to take operational measures before any event could be felt by the population in the area:

- Magnitude > 1.5 and/or PGV > 0.5 mm/s (on 2 seismologic stations minimum) implies a continuous monitoring
- Magnitude > 1.7 and/or PGV > 1 mm/s (on 2 seismologic stations minimum) implies operational measures to be taken such as reduction of plant injection flow rate
- PGV > 1.5 mm/s (on 2 seismologic stations minimum) implies a progressive shut-down

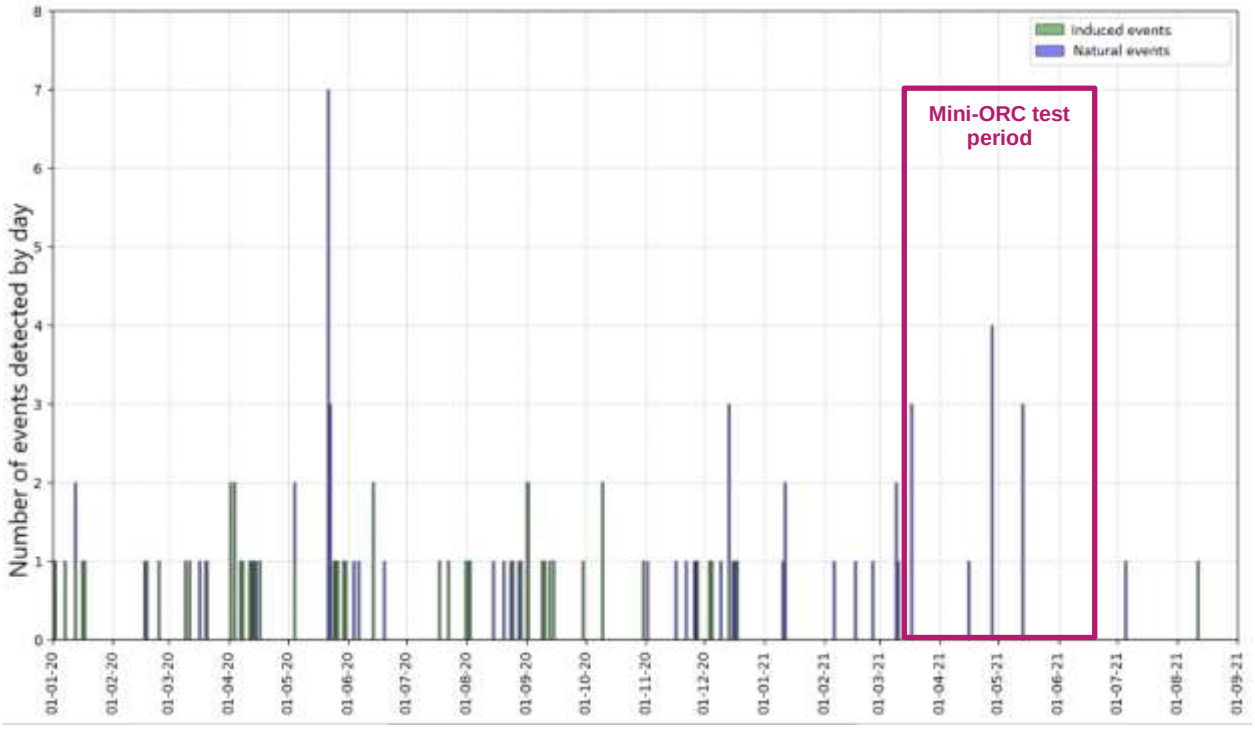

Figure 23: Number of natural and induced events detected by days between 01.2020 and 09.2021.

Figure 24 shows the distribution of the magnitudes of the induced events as a function of time for the 54 significant events detected and located between 01-01-2020 and 01-09-2021. All micro-earthquakes have a magnitude less than 1.5.

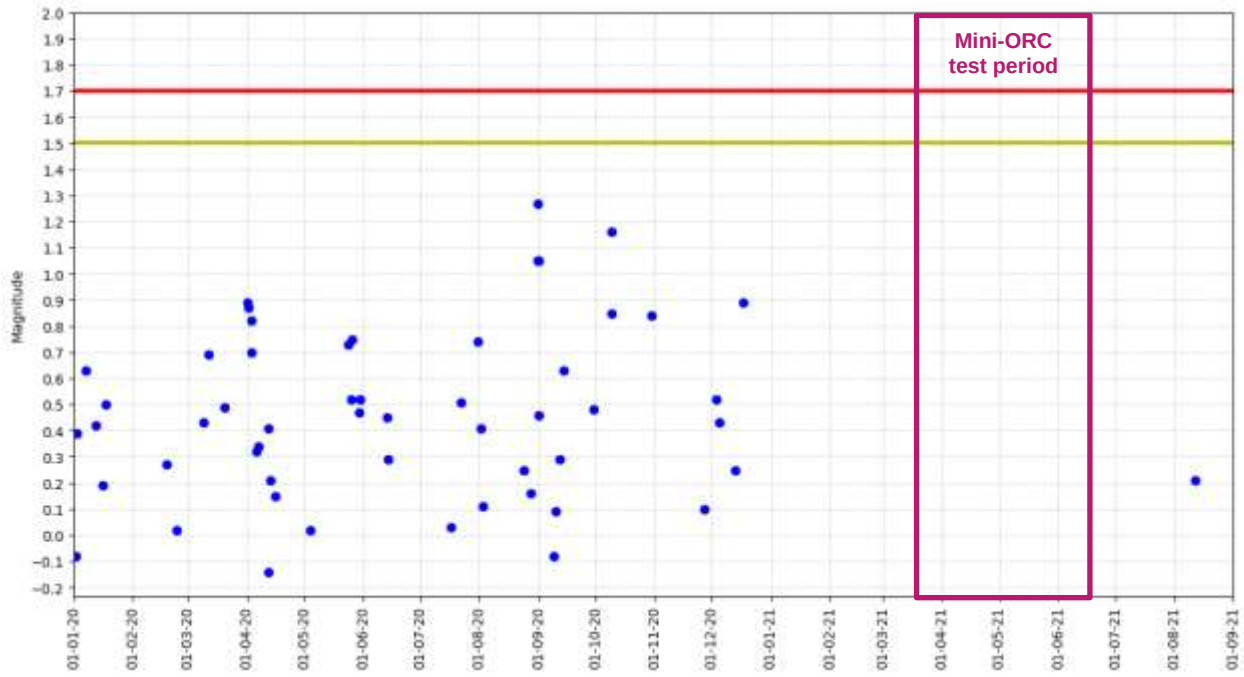

Figure 24: Distribution of the magnitudes of the induced events recorded and detected between 01-01-2020 and 01-09-2021.

Figure 25 shows the distribution as a function of time of the maximums of the PGVs recorded on the vertical and horizontal components of the stations of the monitoring network for the 54 significant events detected and located between 01-01-2020 and 01-09-2021. All the 54 recorded micro-earthquakes have a PGV of less than 0.5 mm/s.

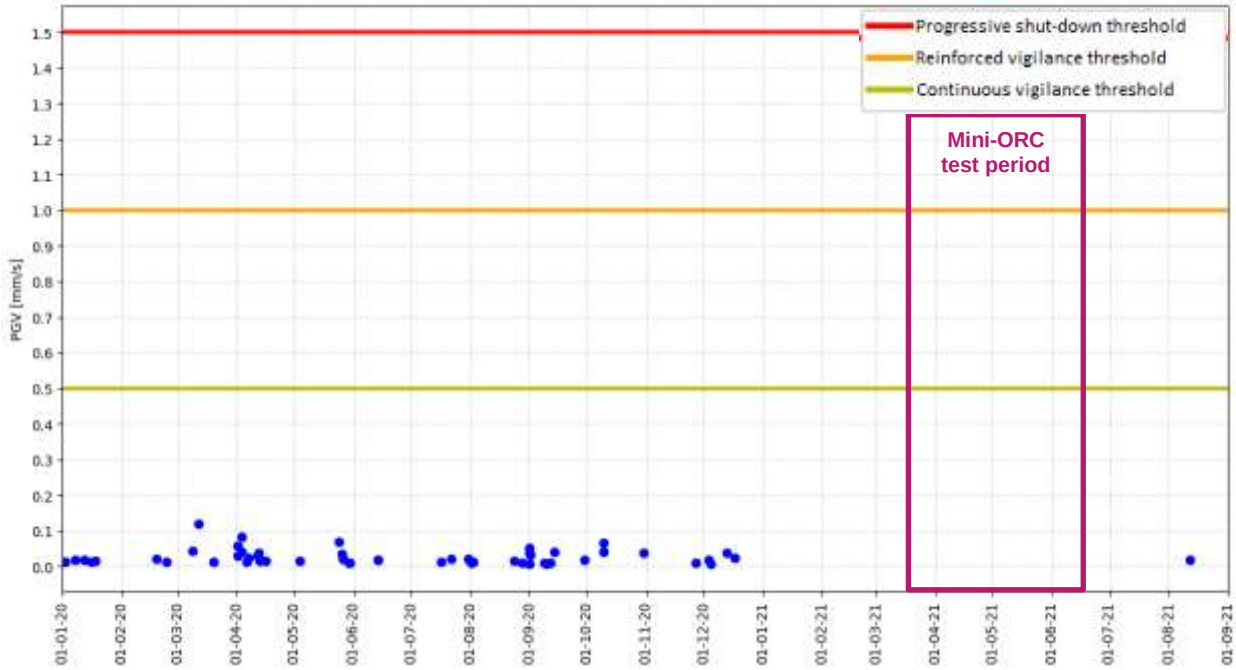

Figure 25: Distribution of PGVs of induced events recorded and detected between 01-01-2020 and 01-09-2021.

During the period of Mini-ORC test, not a single induced event was detected by the densified seismic monitoring network, meaning that this operation is not associated with any rise of the induced micro-seismic activity.

Distributed Fibre Optic Sensing results:

Various campaigns of acoustic acquisition using Distributed Acoustic Sensing (DAS) have been achieved along the fibre optic cable deployed in EPS-1 observation well in Soultz-sous-Forêts since July 2020. However, no seismic event has been recorded during the acquisition periods.

2.4.2 Discussion

During the period of Mini-ORC test, all monitoring devices did not reveal any major changes in the studied physical parameters. We did not notice any variation in the temperature and pressure or in the induced seismic activity in the area which could have been related to the colder reinjection in the geothermal reservoir.

Indeed, it turns out that the Mini-ORC use had no impact on reinjection temperature (Figure 26). Reinjection temperature is mainly controlled by the main power plant ORC efficiency, which is dependent on outdoor temperature, and it seems that the additional ORC power (16kW mean power) is too low in comparison of the main ORC (installed power 1700kW) to produce a significant temperature change of reinjection temperature.

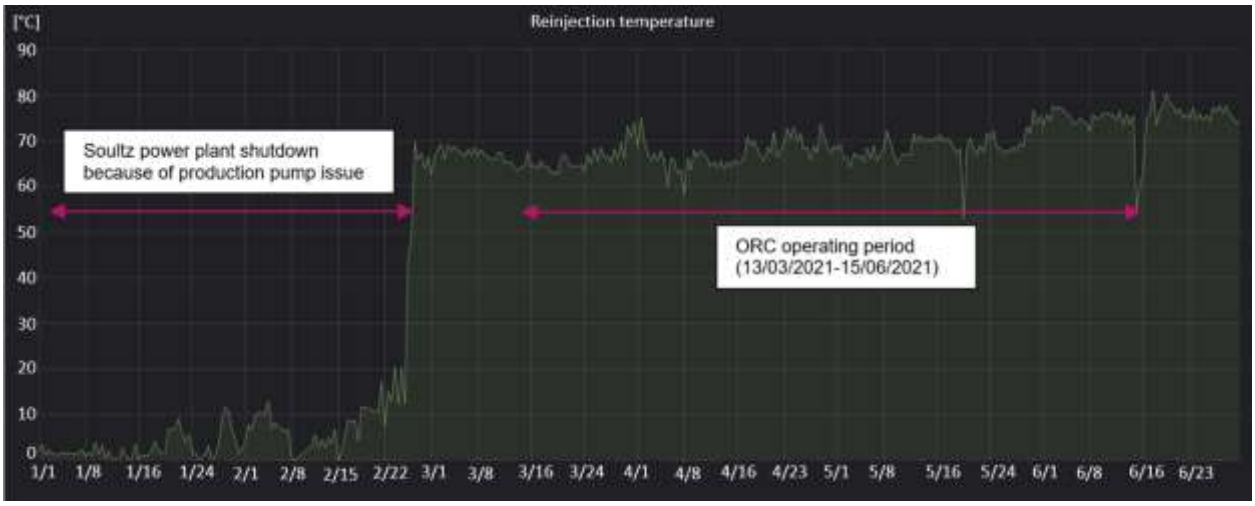

Figure 26: Reinjection temperature in Soultz between 01/01/2021 and 30/06/2021.

If the slight temperature increase visible on Figure 22 corresponds to a real signal, then it could be interpreted as a “hot front” coming in this part of the reservoir due to the long stop of SsF plant between September 2020 and February 2021, while the colder front due to the restart of the plant in February has not reached EPS-1 by May 2021.

2.5 CONCLUSION

This report compiles physical and chemical measurements acquired while performing different on-site tests to assess the feasibility of colder reinjection on the EGS power plant of Soultz-sous-Forêts. 2 colder reinjection tests were performed on this site: one with a small heat exchanger to study scaling precipitation down to 40°C and assess the behaviour of different metallurgies and the other one to test the production of electricity at these low temperatures with a small mobile ORC unit.

The observations and analyses performed on scales formed during the first test highlighted the homogeneity of scale composition below 100°C whatever the metallurgy and the temperature. They are mostly Arsenic-Antimony-rich Lead sulphides of galena type. Whereas silica deposition was the main concern for not reinjecting at temperature lower than 60-70°C, combination of thermodynamic and kinetic modelling of scale formation indicates that the observed absence of silicates in the first test is controlled by kinetic effect, whereas they should have been dominant in regards of pure thermodynamics. This modelling also highlighted the lack of kinetic data at pressure and temperature representative of SsF operational conditions which prevented to further investigate the repartition between metal sulphides. Overall, this first test and subsequent analyses and models shows the feasibility of reinjecting at 40°C regarding scaling issue.

For the second test with a Mini-ORC producing electricity on-site, the monitoring network of SsF plant has been enhanced with 2 additional seismic sensors in surface, 3 piezometers and 1 optic fiber in observation wells. All these sensors have been successfully deployed and were operational for the Mini-ORC test.
Whereas no clear signal related to the Mini-ORC test could be seen with the monitoring network, this cannot attest of the absence of impact on the reservoir of lowering the reinjection temperature down to 40°C. Indeed, the Mini-ORC did not extract sufficient thermal energy to reduce significantly the injection temperature which remained within seasonal variations. Thus, the impact of colder reinjection on the reservoir is only assessed through reservoir modeling presented in MEET deliverable D3.9, Baujard et al, 2021, Mahmoodpour et al, 2021a, Mahmoodpour et al, 2021b (all submitted to Geosciences).
Nevertheless, the successful acquisition and processing of the optic fiber signal in EPS-1 well showed the opportunity to have a powerful monitoring tool capable of measuring acoustic waves and temperature in real time all along the well. For the first time, it also showed very promising results for pressure measurements which needs further developments to become a commercial product.

2.6 REFERENCES

Agemar, T., Schellschmidt, R., and Schulz, R., 2012, Subsurface temperature distribution in Germany: Geothermics, v. 44, p.65–77.

Baillieux, P., Schill, E., Edel, J.-B., Mauri, G., 2013. Localization of temperature anomalies in the Upper Rhine Graben: insights from geophysics and neotectonic activity. Int. Geol. Rev. 55, 1744–1762. http://dx.doi.org/10.1080/00206814.2013.794914.

Baujard, C., Genter, A., Dalmais, E., Maurer, V., Hehn, R., Rosillette, R., ... & Schmittbuhl, J. (2017). Hydrothermal characterization of wells GRT-1 and GRT-2 in Rittershoffen, France: Implications on the understanding of natural flow systems in the Rhine Graben. Geothermics, 65, 255-268.

Baujard, C., Rolin, P., Dalmais, E., Hehn, R., Genter, A., (2021). Soultz-sous-Forêts geothermal reservoir: structural model update and thermo-hydraulic numerical simulations based on 3 years operation data. Geosciences 2021 (submitted).

Bosia C., Mouchot J., Ravier G., Jähnichen S., Degering D., Scheiber J., Dalmais E., Baujard C., Genter A., (2021). Evolution of Brine Geochemical Composition during Operation of EGS Geothermal Plants (Alsace, France), Proceeding of 46th Workshop on Geothermal Reservoir Engineering, Stanford, California, February 15-17, 2021

Evans, K. F., Genter, A., & Sausse, J. (2005). Permeability creation and damage due to massive fluid injections into granite at 3.5 km at Soultz: 1. Borehole observations. Journal of Geophysical Research: Solid Earth, 110(B4).

Gérard, A., Genter, A., Kohl, T., Lutz, Ph., Rose, P., Rummel, F., (2006). The deep EGS (”Enhanced Geothermal Systems”) project at Soultz-sous-Forêts (Alsace, France), Geothermics, Vol. 35, 473-483.

Haas-Nüesch, R.; Heberling, F.; Schild, D.; Rothe, J.; Dardenne, K.; Jähnichen, S.; Eiche, E.; Marquardt, C.; Metz, V.; Schäfer, T. Mineralogical characterization of scalings formed in geothermal sites in the Upper Rhine Graben before and after the application of sulfate inhibitors. Geothermics (2018), 71, 264-273.

Hartog, A. H. (2017). An introduction to distributed optical fibre sensors. CRC press.

Hurtig, E., Grosswig, S., & KÜHN, K. (1997). Distributed fibre optic temperature sensing: A new tool for long-term and short-term temperature monitoring in boreholes. Energy sources, 19(1), 55-62.

Kirknel, I. A., Werger-Gross, T. N., Kann, D. J., Thomsen, K., & Fosbøl, P. L. Thermodynamic modelling of water chemistry in geothermal systems. Proceedings of European geothermal congress 2019, Den Haag, 11-14 june 2019

Kunan, P., Ravier, G., Dalmais, E., Ducousso, M., Cezac, P., (2021). Thermodynamic and Kinetic Modelling of Scales Formation at the Soultz-sous-Forêts Geothermal Power Plant. Geosciences 2021(submitted).

Ledésert, B.A; Hébert, R.L.; Mouchot, J.; Bosia, C.; Ravier, G.; Seibel, O.; Dalmais, E.; Ledésert, M.; Trullenque, G.; Sengelen, X.; Genter, A. Scaling in a Geothermal Heat Exchanger at Soultz-Sous-Forêts (Upper Rhine Graben, France): A XRD and SEM-EDS Characterization of Sulfide Precipitates, Geosciences (2021), 11,271.

Mahmoodpour, S., Singh, M., Turan, A., Bär, K., Sass, I. (2021a). Hydro-thermal modeling for geothermal energy extraction from Soultz-sous-Forêts, France. Geosciences 2021 (submitted).

Mahmoodpour, S., Singh, M., Bär, K., Sass, I. (2021b). Impact of well placement in the fractured geothermal reservoirs 2 based on available discrete fractured system. Geosciences 2021 (submitted).

Mateeva, A., Lopez, J., Potters, H., Mestayer, J., Cox, B., Kiyashchenko, D., ... & Detomo, R. (2014). Distributed acoustic sensing for reservoir monitoring with vertical seismic profiling. Geophysical Prospecting, 62(4-Vertical Seismic Profiling and Microseismicity Frontiers), 679-692.

Mouchot J., Cuenot N., Bosia C., Genter A., Seibel O., Ravier G., Scheiber J.: First year of operation from EGS geothermal plants in Alsace, France: scaling issues, Stanford Geothermal Workshop 2018, Stanford, California, USA, 12-14 February 2018

Pribnow, D., Schellschmidt, R., 2000. Thermal tracking of upper crustal fluid flow in the Rhine Graben. Geophys. Res. Lett. 27.

Sanjuan, B., Millot, R., Innocent, C., Dezayes, C., Scheiber, J., Brach, M., (2016). Major geochemical characteristics of geothermal brines from the Upper Rhine Graben granitic basement with constraints on temperature and circulation. Chem. Geol. 428, 27–47.

Scheiber, J.; Nitschke, F.; Seibt, A.; Genter, A. Geochemical and Mineralogical Monitoring of the Geothermal Power Plant in Soultz-sous-Forêts (France). Proceedings, 37th Workshop on Geothermal Reservoir Engineering, Stanford University, Stanford, California, USA, January 30 - February 1, 2012.

Vidal J., Genter A., (2018). Overview of naturally permeable fractured reservoirs in the Upper Rhine Graben: insights from geothermal wells, Geothermics 74, July 2018, 57-73. https://doi.org/10.1016/j.geothermics.2018.02.003

3 APPENDIX

Version submitted to Geosciences on September 22nd, 2021 of paper “Kunan, P., Ravier, G., Dalmais, E., Ducousso, M., Cezac, P., (2021). Thermodynamic and Kinetic Modelling of Scales Formation at the Soultz-sous-Forêts Geothermal Power Plant. Geosciences 2021(submitted)”.

geosciences

MDPI

Type of the Paper (Article)

Thermodynamic and Kinetic Modelling of Scales Formation at the Soultz-sous-Forêts Geothermal Power Plant

Pierce Kunan [1], Guillaume Ravier [1,*] Eléonore Dalmais [1], Marion Ducousso [2], and Pierre Cezac [2]

[1] Affiliation 1; ES-Géothermie, 5 Rue Ampère 67450 Mundolsheim, France
[2] Affiliation 2; École Nationale Supérieure en Génie des Technologies Industrielles, Bat D'Alembert, Rue Jules Ferry, BP 7511, 64075 PAU Cedex, France
* Correspondence: guillaume.ravier@es.fr

Abstract: Geothermal energy has been a subject of great interest since the 1990's in the Upper Rhine Graben (URG), where the first European Enhanced Geothermal System (EGS) pilot site has been developed, in Soultz-sous-Forêts (SsF), France. Several studies have already been conducted on scales occurring at the reinjection side at the geothermal plants located in the URG. It has been observed that the composition of the scales changes as chemical treatment is applied to inhibit metal sulfate. The purpose of this study is to model the scaling phenomenon occurring in the surface pipes and the heat exchangers at the SsF geothermal plant.

PhreeqC, a geochemical modelling software, was used to reproduce the scaling observations in the geothermal plant during exploitation. A suitable database was chosen based on the availability of chemical elements, minerals, and gas. A thermodynamic model and a kinetic model were proposed for modelling the scaling phenomenon. The thermodynamic model gave insight on possible minerals precipitated while the kinetic model, after modifying the initial rates equation, produced results that were close to the expected scale composition at the SsF geothermal plant. Additional laboratory studies on the kinetics of the scales were proposed to compliment the current model.

Keywords: Upper Rhine Graben, Soultz-sous-Forêts, geothermal brine, scaling, metal sulfides, thermodynamic, kinetics

Citation: Kunan, P.; Ravier, G.; Ducousso, M. ; Cezac, P. ; Thermodynamic and Kinetic Modelling of Scales Formation at the Soultz-sous-Forêts Geothermal Power Plant *Geosciences* **2021**, *11*, x. https://doi.org/10.3390/xxxxx

Academic Editor: Firstname Lastname

Received: date
Accepted: date
Published: date

1. Introduction

1.1. Geothermal energy in the Upper Rhine Graben

The Upper Rhine Graben (URG) is a rifting formation, oriented NNE, part of the European Cenozoic rift system. It extends for 300 km of length, from Basel (Switzerland) in the south to Mainz (Germany) in the north. Important thermal anomalies have been identified in the URG thanks to a rich geological exploration. These anomalies delineate thermal gradient locally over 100°C/km in the first km of sediments and controlled with normal faults parallel to the graben direction. The first European Geothermal research project of Soultz-sous-Forêts (SsF) was conducted initially in the early 90's. This project was based on the Hot Dry Rock (HDR) concept, where the goal was to create an artificial heat exchanger in the basement rocks by hydraulic fracturing [1]. However, the results obtained after the drilling of the first well at SsF showed the presence of natural fluid circulation through the existing fracture network of the reservoir [2]. Since then, the Enhanced Geothermal System (EGS) technology was incorporated into future development of the URG geothermal project. This approach consists of exploiting the natural thermal brine circulation by improving if necessary, the connection between the geothermal wells and the reservoir with various chemical, hydraulic, and thermal treatments [3].

There are several geothermal projects that have been developed in the French, German and Swiss URG region over the past years. In France, two notable geothermal plants are in operation at SsF and Rittershoffen, respectively for power and heat production while in Germany, 3 geothermal plants are in operation for power generation.

1.2. SsF geothermal power plant

The Soultz-sous-Forêts geothermal project started in 1987 and is the cradle of the geothermal energy European research in granitic and fractured systems. Over 30 years of research, the geothermal site at SsF continues to exploit commercially the fractured basement for the EEIG Heat Mining. The actual geothermal system consists of three wells: one production well named GPK-2 and two injection wells named GPK-3 and GPK-4 which are drilled 5 km into the granitic basement. The geothermal brine is produced at a temperature of 150°C, reaching the wellhead with a nominal flow rate of 30 kg/s provided by a downhole production Line Shaft Pump [4]. The installed gross capacity of the binary plant is around 1.7MWe (Figure 1).

Figure 1. The SsF geothermal power plant (Source: EEIG Heat Mining)

The geothermal brine is flowed through a system that consist of three consecutive double pass tubular heat exchangers which supply heat to an Organic Rankine Cycle (ORC) to produce electricity. The geothermal brine is then fully reinjected into the granitic basement at around 70°C. The volume of reinjected brine is split between the two injection wells without the need of reinjection pumps. The well-head overpressure in the surface infrastructure is regulated by using production pump which reaches about 23 bars to keep the gas dissolved in the brine. The reinjection temperature is linked to the conversion process. The geothermal plant has been successfully producing electricity commercially since September 2016, with an availability rate of about 90% for the past four years [5]. The granite reservoir is made of a porphyritic monzogranite rich in K-feldspar megacrysts. Primary silicate minerals are quartz, plagioclase, biotite, and hornblende. A chemical analysis on the composition of the brine was taken in February 2020 (Table 1a, [6]). while an analysis on the gas dissolved in the brine was taken in April 2019 (Table 1b, [6]).

Table 1a. Composition of brine at the production well of the SsF geothermal plant (Bosia et al., 2021).

GPK-2 (Production well)												
Composition of brine (mg/L)	Na	Ca	K	Cl	Mg	Sr	Li	SiO_2	SO_4	Br	Mn	NH_4
	26400	7020	3360	55940	123	422	160	179	108	240	17	23.2
Composition of brine (mg/L)	As	Ba	Cs	Rb	B	Fe	Zn	F	I	Cu	Pb	Cd
	10	26	14	23	38	26.3	2.8	1.3	1.6	0.001	0.11	0.01
Composition of brine (mg/L)	Sb	Al	U	Ni	HCO_3	COT						
	0.06	0.05	0.001	0.0011	197	0.9						

Table 1b. Composition of gas in brine at the production well of the SsF geothermal plant (Bosia et al., 2021).

GPK-2 (Production well)		
Gas dissolved in brine	%vol	Partial pressure (atm)
CO_2	0.882	0.882
N_2	0.0908	0.0908
CH_4	0.0239	0.0239

1.3. Geochemical characterization of the scale during operation

In the Upper Rhine Graben region, the main scales observed related to deep geothermal activity have been studied not only because that when represented at a significant amount of secondary precipitations they could plug the geothermal infrastructures (pipe, heat exchanger, well-head) but also because the scales have the properties to trap radiogenic elements such as 226Ra and 210Pb in their crystalline lattices [7-9]. The main mineral precipitations related to scales are sulfates (barite, celestite), sulfides (galena, pyrite), nanocrystalline intermetallic mixed compound (Sb, As), elemental metals (Pb, As, Sb), oxides metals and carbonates [7,10-11]. Mineralogical and chemical analyses also show the presence of magnetite and sphalerite in the scale deposit [7,12-14]. Occurrences of scales consisting of silicates are quite rare. Locally, laurionite (PbCl (OH)), a hydrothermal lead mineral has been identified [8]. By using sulfate inhibitors, barite precipitation was strongly reduced. However, mainly brittle grey-dark scales precipitating on the pipe walls consisting of PbS, and elemental Pb, As, Sb are precipitating in the geothermal infrastructures. Traces of halite are present on some samples, but it corresponds to a drying residue from the geothermal brine [8]. Based on Raman spectrum of the sulfide phase, a hydrothermal Pb-Sb-Cu-sulfide ($Pb_{13}CuSb_7S_{24}$) has been characterized as well as an amorphous phase [8]. Therefore, in the Upper Rhine Graben, scale formation before the application of sulfate scale inhibitors was dominated by (Ba, Sr, Ca, (Ra))SO_4 solid-solution scalings containing minor amounts of galena or mixed sulfide phases [8].

Recently, Mouchot et al. (2018) [9] conducted a study on the operation at the geothermal plant in the URG region, notably at the SsF geothermal plant. Complementary studies by Mouchot et al. (2019) [5] and Ledésert et al. (2021) [15] reported on the effects of the chemical treatment used to inhibit the formation of sulfate scales at the SsF geothermal plant. This current study aims to create a predictive model for the formation of scales during operation at the SsF geothermal plant. The scaling commonly occurs at the cold side of the SsF geothermal plant [7]. The black scales deposit at the wall of the pipes and

heat exchanger as shown in figure 1. In the framework of the MEET research project, CY Cergy Paris Université conducted a study with a Zeiss GeminiSEM 300 Scanning Electron Microscopy, coupled with a Bruker Energy Dispersive Spectrometry, on different scales found in the test heat exchanger at Soultz-sous-Forêts. Figure 3 details a (Pb,As,Sb)S fibro-radiated hilly scale found at 50°C on 1.4410 stainless steel tube.

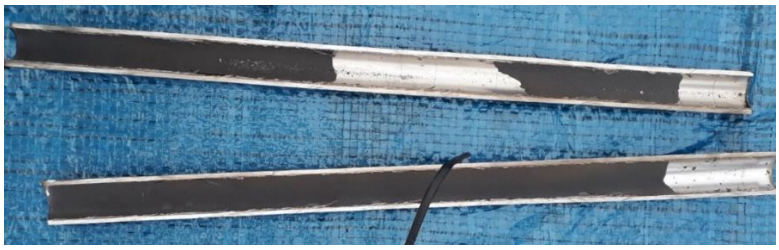

Figure 2. PbS scales deposited in tubes from the test heat exchanger

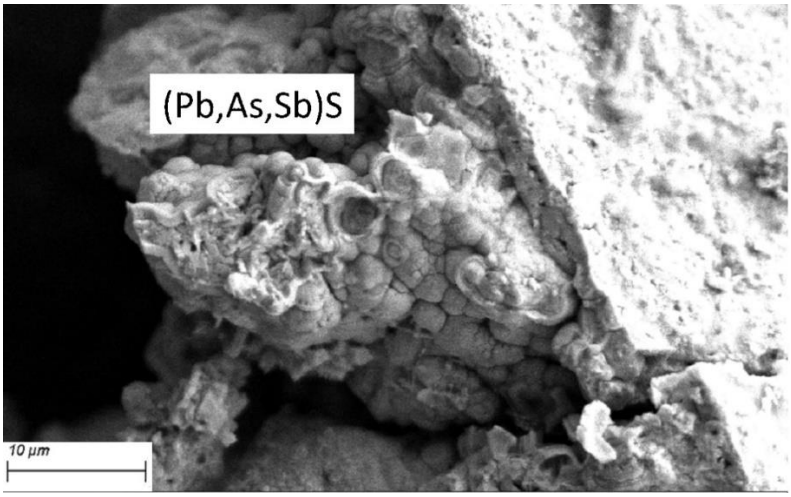

Figure 3. Microscopic photo of (Pb,As,Sb)S scale found at SsF plant (Ledésert et al., 2021)

Scales in the range between 150°C and 65°C have been sampled in June 2018 before cleaning operation in the ORC evaporator and preheaters after nearly 1 year of operation. Chemical composition of these scales has been determined using ICP MS method which is a type of mass spectrometry that uses an inductively couple plasma to ionize the sample. Scales in the range between 60°C and 40°C have been sampled in April 2019 in a test heat exchanger (HEX) designed with different metallurgy and installed at the SsF geothermal plant during 3 months in the framework of the MEET research project [16]. The latest chemical composition of scales observed at SsF geothermal plant within a range of temperature between 150°C to 40°C are presented in table 2. Table 2 considers only scaling samples from tubes with 1.4410 metallurgy like the ORC heat exchanges to have a good comparison. A detail description of these scales is given by Ledésert et al. (2021) [15], and chemical composition was also determined using ICP MS method. Chemical treatment of the brine was almost the same for the two sets of scales. These scales consist of S, Pb, Sr, Ba, Sb, As, Fe, Si, and Cu elements.

Table 2.The mass composition of scales formed in the heat exchangers at the geothermal plant and in the test heat exchangers in percentage

Temperature	S	Pb	Sr	Ba	Sb	As	Fe	Si	Cu	Exchanger
150	2.9%	2.0%	2.9%	0.94%	0.11%	0.53%	1.7%	3.8%	0.40%	ORC Inlet Evaporator
120	10.4%	13.0%	0.73%	0.61%	1.1%	4.2%	4.0%	6.2%	15.1%	ORC Outlet Evaporator
120	11.8%	26.5%	0.65%	1.9%	3.3%	6.6%	7.5%	8.0%	16.6%	ORC Inlet Preheater
90	11.2%	36.1%	0.86%	3.6%	3.1%	5.2%	8.0%	16.9%	5.1%	ORC Preheater
65	13.1%	46.3%	0.51%	2.2%	6.3%	7.3%	4.6%	8.4%	4.5%	ORC Outlet Preheater
60	13.1%	74.6%	0.01%	0.00%	6.4%	3.2%	0.07%	1.4%	0.40%	Test HEX
50	14.4%	66.5%	0.01%	0.01%	11.4%	4.3%	0.55%	1.0%	0.43%	Test HEX
40	16.7%	64.2%	0.01%	0.01%	10.9%	4.5%	0.48%	1.6%	0.36%	Test HEX

The presentation of the mass percentage of scales is based on the total elements found in the scales. Certain compounds, mainly carbonates, were omitted from Table 2 because they are not the main focus of this study which is dedicated to low temperature scale formation. There are also lesser amounts of the scales deposited in the higher temperatured heat exchangers (ORC heat exchangers) while more scales are deposited in the lower temperatured heat exchangers (Test HEX).

Lead is found primarily at lower temperatures notably at temperatures below 120 °C. Sulfur, arsenic, silicon, and antimony are also deposited at large quantities after lead. The rest of the elements are found in smaller traces (less than 5%). The test heat exchanger has a different concentration of scales compared to the ORC heat exchangers at the geothermal plant due to the difference in temperature. In the test heat exchanger, lead has a higher concentration than those in the main exchangers. The chemical treatment on the sulfate scales proved to be effective as the quantity of barium sulfate (barite) and strontium sulfate (celestite) are found in very small quantities which are less than 4% for any point of temperature.

The main objective of this study is to model the scaling phenomenon occurring in the surface pipes and heat exchangers at the SsF plant. Therefore, these geochemical analyses would serve as references for comparing with the modelling results of the formation of the scales.

2. Methods

The modelling of the geochemical fluids is done through the software, PhreeqC which is a computer program that is written in C++ programming language. It is designed to perform numerous aqueous geochemical calculations. PhreeqC implements several types of aqueous models depending on the database used. This program was created by the U.S. Geological Survey (USGS). PhreeqC is freely distributed by the USGS and is currently an open source software.

PhreeqC uses a pre-established thermodynamic database to perform the calculations during modelling of a fluid. Each database has different sets of elements and aqueous species as well as different thermodynamic data which are taken from different references sources. There are several databases found within the installation of the PhreeqC program. Supplementary databases were also found in the PhreeqC Users forum. There are databases taken from studies such as e THERMOCHIMIE [17] and THEREDA [18]. The PhreeqC manual [19] was referred to when performing the modelling of formation of scales with PhreeqC. Table 3 shows the list of databases gathered which are listed from D1 to D19:

Table 3. PhreeqC databases and allocated nomenclature

Databases	Nomenclature
Phreeqc	D1
Pitzer	D2
ColdChem	D3
Core10	D4
Frezchem	D5
Iso	D6
LLNL	D7
MINTEQ	D8
Minteq v4	D9
Pitzer_Old	D10
sit	D11
T_H	D12
WATEQ4F	D13
Thermoddem_06_2017	D14
PHREEQC_ThermoddemV1.10_15Dec2020	D15
ThermoChimie_PHREEQC_eDH_v9b0	D16
THEREDA_2020_PHRQ	D17
CEMDATA18.1-16-01-2019-phaseVol	D18
ThermoChimie_PhreeqC_SIT_oxygen_v10a	D19

2.1. Verification: Elements

In order to verify the validity of the databases to be used in the modelling process, the sets of elements available within the databases were compared to the elements found in the geothermal fluid at the SsF plant. The latest chemical analysis (taken in February 2020) on the composition of the brine at the SsF plant was used to cross-reference with the sets of elements found in the databases to narrow down the list of valid databases. This analysis showed that there was high concentration of Na and Cl ions in the brine. The recent study by Bosia et al. (2021) [6] provides further details on the geochemical dataset used.

Databases with more supplementary elements were taken more into consideration due to the likelihood of simulating the actual fluid. Thus, the presence of the elements in the databases are compared to the elements found in the geothermal fluid at the SsF plant (Table 4)

Table 4. Geochemical elements in the databases. * = limited 199

	D1	D2	D3	D4	D5	D6	D7	D8	D9	D10	D11	D12	D13	D14	D15	D16	D17	D18	D19
S	x	x	x	x	x	x	x	x	x	x	x	x	x	x	x	x	x	x	x
Pb	x						x	x	x		x	x	x	x	x	x			x
Sr	x	x					x	x	x	x	x	x	x	x	x	x	x	x	x
Ba	x	x					x	x	x	x	x	x	x	x	x	x			x
Sb							x	x	x		x			x	x	x			x
As							x	x	x		x	x	x	x	x	x			x
Fe	x	x		x		x	x	x	x	x	x	x	x	x	x	x		x	x
Si	x	x		x		x	x	x	x		x	x	x	x	x	x	x	x	x
Cu	x			x			x	x	x		x	x	x	x	x	x			x
Al	x			x		x	x	x	x		x	x	x	x	x	x	x	x	x
B	x	x		x			x	x	x	x	x	x	x	x	x	x			x
Be							x	x	x					x	x				
Br	x	x				x	x	x	x	x	x	x	x	x	x	x			x
Ca	x		x	x	x	x	x	x	x	x	x	x	x	x	x	x	x	x	x
Cd	x						x	x	x		x	x	x	x	x	x			x
Ce							x							x	x				
Cl	x	x	x	x	x	x	x	x	x		x	x	x	x	x	x	x	x	x
Co				x			x		x		x			x	x	x			x
Cs							x				x	x	x	x	x	x	x		x
Dy							x							x	x				
Er							x							x	x				
Eu				x			x				x			x	x	x			x
F	x					x	x	x	x		x	x	x	x	x	x			x
Gd				x			x							x	x				
Ge														x	x				
Hg							x	x	x		x			x	x	x			
Ho							x				x			x	x	x			x
I							x	x	x		x	x	x	x	x	x			x
In							x							x	x				
K	x	x	x	x	x	x	x	x	x	x	x	x	x	x	x	x	x	x	x
La							x							x	x				
Li	x	x		x			x	x	x	x	x	x	x	x	x	x			x
Lu							x							x	x				
Mg	x	x	x	x	x	x	x	x	x	x	x	x	x	x	x	x	x	x	x
Mn	x	x		x			x	x	x	x	x	x	x	x	x	x			x
Mo				x			x		x		x			x	x	x			x
Na	x	x	x	x	x	x	x	x	x	x	x	x	x	x	x	x	x	x	x
Nd							x							x	x		x		
Ni				x			x	x	x		x		x	x	x	x			x
P	x			x		x	x	x	x		x	x	x	x	x	x	x		x
Pd							x				x			x	x	x			x
Pr							x							x	x				
Rb							x	x			x	x	x	x	x	x			x
Re							x							x	x				
Rh														x	x				
Sc				x			x							x	x				
Sm				x			x				x			x	x	x			x
Tb							x							x	x				
Tm							x							x	x				

W		x					x							x	x				
Y							x							x	x				
Yb							x							x	x				
Zn	x	x		x			x	x	x		x	x	x	x	x	x			x
HCO_3	x	x		x	x	x	x	x	x	x	x	x	x	x	x	x*	x	x	x
NH_4				x			x	x	x		x	x	x	x	x	x		x	x
SO_3				x			x	x	x		x	x*	x*	x	x	x		x	x
SO_4	x	x	x	x	x	x	x	x	x	x	x	x	x	x	x	x	x	x	x
Total	23	17	7	26	8	14	55	32	33	14	38	29	30	57	57	38	14	14	37

The geochemical elements from the table 4 are represented in their aqueous state. From this study, the Thermoddem (D14 and D15) [20] and LLNL (D7) [21] databases, having respectively 57 and 55 elements of the 57 SsF brine chemical composition, are observed to be suitable for the purpose of this study as they possess the most amount elements found in the brine at the SsF plant. Further reference to the Thermoddem database will be the Thermoddem (D15) database instead of the Thermoddem (D14) database because D15 is the latest version for the Thermoddem database.

2.2. Verification: Minerals

Another criterion set for the validation of the databases is the formation of probable minerals in the geothermal fluid at the SsF plant. A list of known minerals precipitated was made to compare to the minerals found in the databases. Furthermore, a list of probable minerals precipitated was made for minerals that has not been identified before in previous studies. These minerals that are susceptible to precipitation are identified by listing out minerals from the databases that consist of at least two of nine elements that are the majority in the analysis of scales conducted at the site. The nine principal elements are sulfur, lead, strontium, barium, antimony, arsenic, iron, silicon, and copper. A similar approach to the verification of elements was used in the verification of minerals in which a table with the list of minerals was cross-referenced with the database. The occurrences of known minerals and minerals susceptible to precipitation in the databases are tabulated (Table 5).

Table 5. Minerals in the databases

Known Minerals		Databases																		
		D1	D2	D3	D4	D5	D6	D7	D8	D9	D10	D11	D12	D13	D14	D15	D16	D17	D18	D19
Galena	PbS							x	x	x		x	x	x	x	x	x			x
Quartz	SiO_2	x	x		x		x	x	x	x		x	x	x	x	x	x	x	x	x
Calcite	$CaCO_3$	x	x		x	x	x	x	x	x	x	x	x	x	x	x	x		x	x
Anhydrite	$CaSO_4$	x	x	x	x	x	x	x	x	x	x		x	x	x	x	x		x	x
Gypsum	$CaSO_4{:}2H_20$	x	x	x	x	x	x	x	x	x	x	x	x	x	x	x	x		x	x
Barite	$BaSO_4$	x	x					x	x	x	x		x	x	x	x	x			x
Halite	NaCl	x	x	x	x	x	x	x	x	x	x	x	x	x	x	x	x	x		x
Goethite	FeOOH	x			x		x	x	x	x		x	x	x	x	x	x		x	x
Celestite	$SrSO_4$	x	x					x	x	x	x	x	x	x	x	x	x		x	x
Arsenopyrite	FeAsS							x							x	x				
Stibnite	Sb_2S_3							x	x	x		x			x	x	x			x
Possible Other Minerals																				
Hematite	Fe_2O_3	x			x		x	x	x	x		x	x	x	x	x	x		x	x
Strontianite	$SrCO_3$	x						x	x	x		x	x	x	x	x	x		x	x
Svanbergite	$SrAl_3(PO_4)(SO_4)(OH)_6$														x	x				
$Sr_3(AsO_4)_2$	$Sr_3(AsO_4)_2$							x				x			x	x	x			x
SrS	SrS							x				x			x	x	x			x
Anglesite	$PbSO_4$	x						x	x	x		x	x	x	x	x	x			x
Cerussite	$PbCO_3$	x						x	x	x		x	x	x	x	x	x			x
Alamosite	$PbSiO_3$							x	x			x	x	x	x	x	x			x
Beudantite	$PbFe_3(AsO_4)_2(OH)_5{:}H_2O$														x	x				
Corkite	$PbFe_3(PO_4)(OH)_6SO_4$							x							x	x				
Cotunnite	$PbCl_2$							x	x	x		x	x	x	x	x	x			x
Duftite	$PbCuAsO_4(OH)$														x	x				
Hinsdalite	$PbAl_3(PO_4)(SO_4)(OH)_6$							x	x	x			x	x	x	x				
Hydrocerus-site	$Pb_3(CO_3)_2(OH)_2$							x		x		x	x	x	x	x	x			x
Jarosite (Pb)	$Pb_{0.5}Fe_3(SO_4)_2(OH)_6$														x	x				
Lanarkite	$Pb2SO_5$							x	x	x		x	x	x	x	x	x			x
Mimetite	$Pb_5(AsO_4)_3Cl$														x	x				
$Pb_3(AsO_4)_2$	$Pb_3(AsO_4)_2$								x	x		x	x	x			x			x
Pb_3SO_6	Pb_3SO_6							x	x	x			x	x						
$Pb_4(OH)_6SO_4$	$Pb_4(OH)_6SO_4$								x	x			x	x						
Pb_4SO_7	Pb_4SO_7							x	x	x			x	x						
$PbSO_4(NH_3)_2$	$PbSO_4(NH_3)_2$							x												
$PbSO_4(NH_3)_4$	$PbSO_4(NH_3)_4$							x												
Pb(Thiocya-nate)$_2$	$Pb(SCN)_2$							x												
Philipsbornite	$PbAl_3(AsO_4)_2(OH)_5{:}H_2O$														x	x				
Tsumebite	$Pb_2Cu(PO_4)(SO_4)OH$							x							x	x				
Realgar	AsS							x	x	x		x	x	x	x	x	x			x
Orpiment	As_2S_3							x	x	x		x	x	x	x	x	x			x
Bornite	Cu_5FeS_4				x			x							x	x				
Chalcocite	Cu_2S				x			x	x	x			x	x	x	x				
Berthierite	$FeSb_2S_4$														x	x				
	Total	12	7	3	9	4	7	33	25	25	6	21	25	25	35	35	23	2	8	23

The similar conclusion as before can be drawn from this verification in which the two databases, Thermoddem (D15) and LLNL (7) are suitable for the modelling of the geothermal fluids at the SsF plant due to possessing an extensive amount of thermodynamic data on known mineral found as deposits in the plant as well as possible minerals precipitated. The LLNL database has 33 mineral datasets out of the 42 possible minerals deposited while the Thermoddem database has 35 out of the 42 possible minerals deposited.

Another step was carried out to verify the domain of validity for the minerals in the LLNL and Thermoddem databases. The range of temperature valid for each mineral was verified to ensure it corresponds with the maximum modelling temperature of 200°C. For the Thermoddem database, the thermodynamic data of all the minerals are valid within 0°C to 300°C. On the other hand, the LLNL database has different limits for each mineral. Fortunately, the minerals that were identified in table 5 are well within the limits proposed in the LLNL database as the lowest maximum temperature for the minerals found is at 200°C.

2.3. Verification: B-Dot model Database

The two databases of interest, the Thermoddem database and the LNLL database, utilize the B-Dot equation for the calculation of activity of the elements. The B-dot model is also known as the Truesdell-Jones model (TJ model). The ionic strength of the fluid was calculated from the major elements mentioned in the most recent published geochemical datasets in Bosia et al. (2021) [6] and found to be at 1.79 mol/kg for GPK-2 and at 1.8 mol/kg for GPK-3 (Table 6). The unit for the ionic strength can be represented as mol/L or mol/kg since the fluid is primarily composed of water while the effects of the ions in the conversion can be ignored due to their miniscule presence in the fluid. The validity of the B-dot model is verified in figure 1 as the ionic strength is well within the limit of the TJ model for both wells. The higher the ionic strength, the less accurate the results produced.

When the ionic strength of the brine exceeds the limits of the TJ model (2.2 mol/kg), the results obtained from using the B-dot databases will no longer be valid (Figure 4). Since the ionic strength of the fluids at the SsF geothermal plant are well within the limits of the zone of validity, the two databases are thus used for the modelling of the fluids. Furthermore, they are also the most documented in terms of the geochemical elements and minerals.

Table 6. Ionic strength calculations of the geothermal fluid sampled at GPK-2 & GPK-3

	Molar Mass	**GPK-2**	**GPK-3**	**GPK-2**	**GPK-3**	**GPK-2**	**GPK-3**
	M(mg/mol)	mg/L		mol/L		Ionic Strength, I (mol/L or mol/kg)	
Na	23000	26400	26700	1.148	1.161	0.574	0.580
Cl	35500	57490	57490	1.619	1.619	0.810	0.810
K	39100	3350	3350	0.086	0.086	0.043	0.043
Ca	40100	7020	7030	0.175	0.175	0.350	0.351
Sr	87620	422	434	0.005	0.005	0.010	0.010
Br	79904	240	234	0.003	0.003	0.002	0.001
Li	6940	160	163	0.023	0.023	0.012	0.012
SiO_2	40100	179	180	0.004	0.004		
Total		95261	95581	3.063	3.077	1.799	1.807

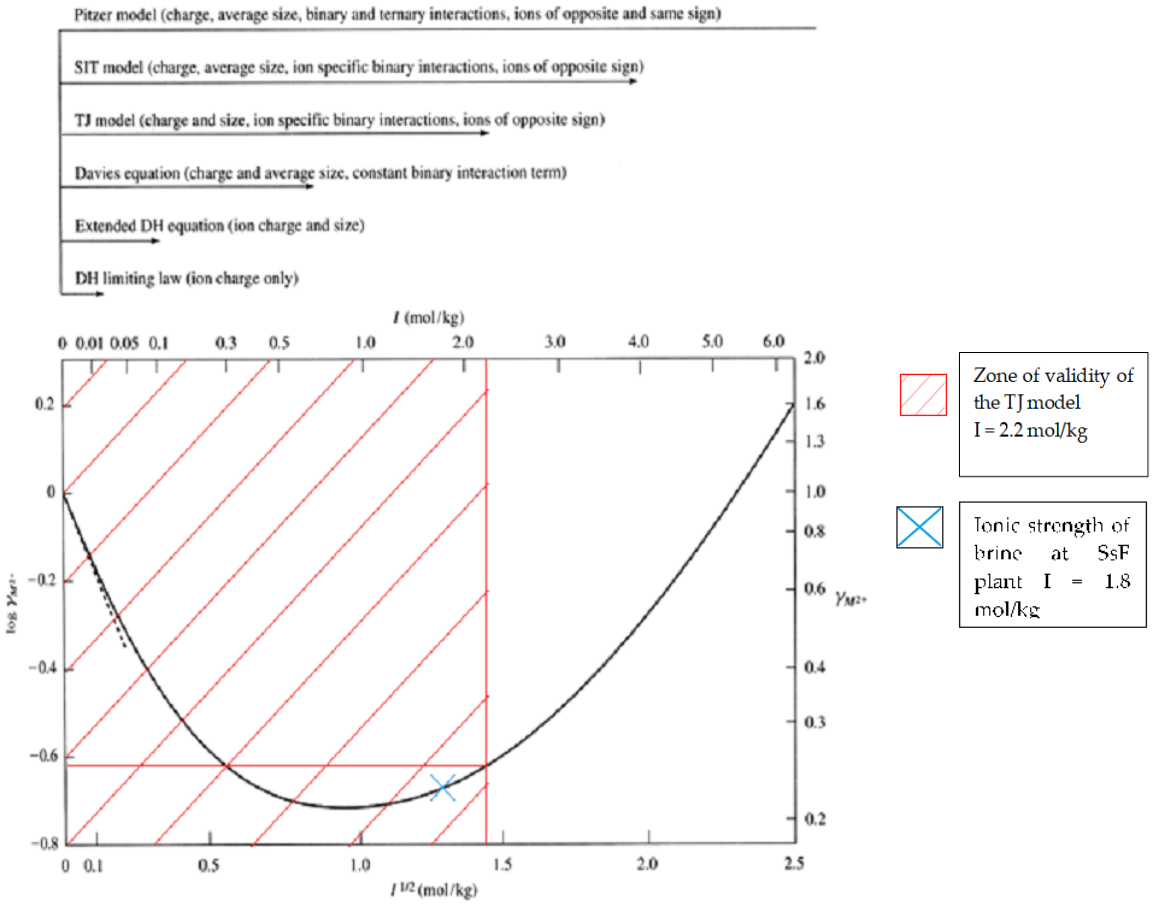

Figure 4. Schematic plot showing the general applicability of different activity coefficient models as a function of ionic strength for a divalent cation. The dashed tangent to the curve at its origin is a plot of the Debye-Hückel limiting law for the ion. (Langmuir, 1997)

2.4. Verification: Gas

The data available on the gases in the databases are compared to those required for modelling the geothermal fluid. The databases are then analyzed by initiating a preliminary modelling of the fluids to compare the results of the modelling with the results at the plant. For this preliminary modelling, the mixture of the gas dissolved in the brine (Table 1b) was used. The conditions of the preliminary modelling are done at pH 5.2 and at two different temperatures, 80°C and 150°C. The saturation pressure of each database is compared and analyzed. For this analysis, the Thermoddem database, the LLNL database and the Pitzer database were used. For the Thermoddem database and the LLNL database, as they were deemed suitable for the modelling of scales through the verification of elements and minerals, they are thus analyzed for the verification of gases. Even though the Pitzer database lacks several data on the elements and minerals, it is still considered for modelling of dissolved gases in the geothermal fluid because this database uses a different model for the calculation of activity of the elements. This may then give a more accurate result in the modelling of dissolved gases in the geothermal fluid. The results of the preliminary modelling at two different temperatures steps in terms of saturation pressure with the three databases are recorded in table 7.

Table 7. Results of the saturation pressure of SsF gas for each database at 2 temperature steps

Temperature(°C)	Pitzer	LLNL	Thermoddem
80	14 atm	10 atm	10 atm
150	18 atm	15 atm	16 atm

The LLNL and Thermoddem databases give out a similar result at both tested temperature while the Pitzer database shows a higher pressure compared to the two previous databases (Table 7). The saturation pressure obtained from modelling at 150°C with the Pitzer database (18 atm = 18.2 bar) is closer to the actual case observed at the SsF plant [23] at the same temperature which ranges between 18.0 and 18.5 bar at relative pressure. The Thermoddem and LLNL databases provided results outside the range of saturation pressure observed at the SsF plant. Thus, the Pitzer database is found to be more suitable than the Thermoddem and LLNL databases for the gas modelling of the SsF plant.

Overall, the Thermoddem database was selected for the modelling of the formation of scales in the geothermal fluids as this database has more data than the LLNL database on the geochemical elements and possible minerals precipitated. Furthermore, the Thermoddem database has been compiled by a French geological survey company, BRGM which is specifically designed for waste derived from natural fluid precipitation [20]. As for modelling of the dissolved gas in the fluid, the Pitzer database was observed to have given a more satisfactory result as mentioned in the previous paragraph. Thus, this database should be used when the observing the solubility of gas in the geothermal fluid.

2.5. Scale Modelling

When modelling the formation of scales with PhreeqC, the physical properties of the fluids such as the temperature, pressure and pH of the fluid are inputted into the software. The initial temperature, pressure and pH of the fluid are 25°C, 1 bar, and pH 5.2 respectively representative of the laboratory conditions for brine analysis. The temperature and pressure were later changed to the production conditions of the brine at the SsF geothermal plant which are at 150°C and 20 bars respectively. The pH of the fluid is also adjusted by the software to reflect the temperature and the composition of the fluid, thus there was no need to modify it. The unit for the concentration of each component in the fluids are also user-defined. In the case of this study, the unit used is in mg/kgw where kgw stands for a kilogram of water. Thus, the unit mg/kgw is the mass in milligrams of the element for each kilogram of water.

The formation of scales at the SsF plant is initially modeled by using thermodynamic modelling. This method uses the thermodynamic database researched in the previous section. The saturation index of each mineral is studied in this modelling process. For any minerals with a saturation index equal or higher than zero for the conditions of the fluid at the geothermal plant, that mineral can potentially precipitate. The amount of minerals precipitated was then calculated. This method provided insight on the potential minerals that could precipitate aside from the minerals already observed in previous studies such as those mentioned in Sanjuan et al. (2011) [10], Scheiber et al. (2012) [7], and Nitschke (2012) [11]. However, this method is limited to cases where thermodynamic equilibrium is reached.

Kinetic modelling was also considered to represent accurately the situation of the formation of scales at the geothermal plant. For this method, the amount of time that the fluids pass through the plant's exchangers is needed. It takes around 3 minutes for the fluid to circulate from the entrance of the first ORC heat exchanger to the exit of the final ORC heat exchanger. In these conditions, the kinetics of the reaction is also a crucial factor

for the kinetic modelling. The kinetic data for chalcopyrite, galena, orpiment, and pyrite was taken from the database made by Zhang et al. (2019) [24]. The kinetic constant for stibnite was taken from Biver et al. (2011) [25] and adjusted into a modified kinetic equation for galena. For other minerals without any kinetic data, a modified kinetic equation of a similar mineral was used. The amount of minerals precipitated is calculated using its kinetic equation. This method refers to the saturation index of the mineral before calculating with the kinetic information available. As stated before, when the saturation index of the mineral is below zero, the kinetic calculation is skipped as the mineral does not precipitate. The duration for the kinetic modelling at each temperature was set to one minute because the velocity of the brine is estimated to be slightly less than 1m/s and the length of the tubes of heat exchanger at 30m. This gives a duration of about 30 seconds to pass through a heat exchanger. Another 30 seconds was added to take into account the head cover and the pipes between each heat exchanger.

3. Results

As mentioned in the previous section, the modelling of scales in the geothermal fluids was done in Phreeqc with the Thermoddem database. For this modelling sequence, the range of temperature and pressure were set. The temperature starts from 150°C which is the highest observable temperature at the SsF plant. The temperature then reduces until the lowest temperature found in the test heat exchanger which is at 40 °C. Additionally, two fictional temperatures were added which are at 175 °C and 200 °C in order to simulate the influence of such high temperatures on the formation of scales. These two temperatures are representative of temperatures found in the geothermal reservoir that is four to five kilometers deep under. The pressure was then fixed at 20 bars to simulate the exact conditions at the SsF geothermal plant.

3.1. Thermodynamic modelling

The precipitation of the minerals was first studied through the observation made on the saturation index of each mineral. For the minerals with a saturation index equal or higher than zero, they are minerals that could possibly be present in the scales at thermodynamic equilibrium (Appendix A, Table A1). A list of potential minerals present within the set range of temperature was constructed from the observation of the saturation index of each mineral (Table 8).

Table 8. Presence of potential minerals at the set range of temperature according to saturation index.

Pressure (bar)		**20**								
Temperature (°C)		40	50	60	65	90	120	150	175	200
Known Minerals										
SiO_2	Amorphous_silica	x	x	x	x	x	x			
$CaSO_4$	Anhydrite								x	x
Sb_2S_3	Stibnite	x	x	x	x	x	x	x		
FeAsS	Arsenopyrite				x	x	x			
$BaSO_4$	Barite	x	x	x	x	x	x	x	x	x
$CuFeS_2$	Chalcopyrite(alpha)	x	x	x	x	x	x	x	x	x
PbS	Galena	x	x	x	x	x	x	x	x	x
SiO_2	Quartz(alpha)	x	x	x	x	x	x	x	x	x
SiO_2	Quartz(beta)	x	x	x	x	x	x	x	x	x
Possible Other Minerals										
$Cu_{1,75}S$	Anilite	x	x	x	x					
$FeSb_2S_4$	Berthierite	x	x	x	x	x	x			
Cu_5FeS_4	Bornite(alpha)	x	x	x	x	x	x	x		
SiO_2	Chalcedony	x	x	x	x	x	x	x	x	x
Cu_2S	Chalcocite(alpha)	x	x	x	x					
SiO_2	Coesite(alpha)	x	x	x	x	x	x			
CuS	Covellite	x	x	x	x					
SiO_2	Cristobalite(alpha)	x	x	x	x	x	x	x	x	x
SiO_2	Cristobalite(beta)	x	x	x	x	x	x	x	x	
$Cu_{1,934}S$	Djurleite	x	x	x	x					
$Fe_{10}S_{11}$	$Fe_{10}S_{11}$						x	x	x	x
$Fe_{11}S_{12}$	$Fe_{11}S_{12}$						x	x	x	x
$Fe_{7,016}S_8$	$Fe_{7,016}S_8$					x	x	x	x	x
Fe_9S_{10}	Fe_9S_{10}						x	x	x	x
FeS_2	Marcassite	x	x	x	x	x	x	x	x	x
As_2S_3	Orpiment	x	x	x	x	x				
FeS_2	Pyrite	x	x	x	x	x	x	x	x	x
$Na_2(Fe_3Fe_2)Si_8O_{22}(OH)_2$	Riebeckite									x

Table 9. Mineral precipitated for thermodynamic modelling (For 40°C – 200°C)

Known Minerals			
Minerals precipitated according to saturation index		**Minerals considered for thermodynamic modelling**	
SiO_2	Amorphous silica	$CuFeS_2$	Chalcopyrite(alpha)
$CaSO_4$	Anhydrite	PbS	Galena
$BaSO_4$	Barite	Sb_2S_3	Stibnite
$CuFeS_2$	Chalcopyrite(alpha)		
PbS	Galena		
SiO_2	Quartz(alpha)		
SiO_2	Quartz(beta)		
Sb_2S_3	Stibnite		
Possible Other Minerals			
Minerals precipitated according to saturation index		**Minerals considered for thermodynamic modelling**	
$Cu_{1,75}S$	Anilite	$Cu_{1,75}S$	Anilite
$FeSb_2S_4$	Berthierite	$FeSb_2S_4$	Berthierite
Cu_5FeS_4	Bornite(alpha)	Cu_5FeS_4	Bornite(alpha)
SiO_2	Coesite(alpha)	CuS	Covellite
CuS	Covellite	FeS_2	Marcasite
SiO_2	Cristobalite(beta)	A_s2S_3	Orpiment
FeS_2	Marcasite	FeS_2	Pyrite
A_s2S_3	Orpiment		
FeS_2	Pyrite		

The next step for the modelling of scales formation at the SsF geothermal plant is to calculate the quantity of minerals precipitating in the given temperature range. An initial modelling based on the present minerals (Table 8) were done and the results showed that not all minerals with a positive saturation index precipitated (Table 9, left side). This is explained by the higher saturation index of several minerals which have higher priority to precipitate. The results of the thermodynamic modelling (Table 10) from using the minerals of the left side of Table 9 showed that majority of the minerals consist of silicates because of the high concentration of O and Si. At the range of temperature between 40°C to 150°C, silicate scales are not usually found at high amounts at the SsF geothermal plant.

Table 10. Results of first thermodynamic modelling in weight percentage

		Temperature (°C)								
	M(g/mol)	40	50	60	65	90	120	150	175	200
As	74.922	0.00%	0.00%	0.00%	0.00%	0.00%	0.00%	0.00%	0.00%	0.00%
Ba	137.33	2.3%	2.1%	4.4%	4.8%	5.1%	5.5%	4.9%	0.00%	0.00%
Ca	40.08	0.00%	0.00%	0.00%	0.00%	0.00%	0.00%	0.00%	5.0%	9.7%
Cu	63.546	0.00%	0.00%	0.00%	0.00%	0.00%	0.00%	0.00%	0.00%	0.00%
Fe	55.847	0.60%	0.52%	0.45%	0.65%	1.3%	1.4%	1.4%	1.2%	1.1%
O	15.999	51.6%	51.7%	50.8%	50.4%	49.5%	49.3%	49.5%	50.8%	49.9%
Pb	207.2	0.01%	0.01%	0.02%	0.00%	0.02%	0.00%	0.01%	0.00%	0.01%
S	32.066	1.2%	1.1%	1.5%	1.9%	2.7%	2.9%	2.7%	5.4%	9.0%
Sb	121.75	0.01%	0.01%	0.02%	0.01%	0.02%	0.02%	0.01%	0.00%	0.00%
Si	28.086	44.3%	44.5%	42.8%	42.3%	41.3%	41.0%	41.4%	37.6%	30.3%

To have a better focus on the modelling of scales at the SsF geothermal plant, the minerals considered for the thermodynamic model was then identified (Table 9, right side). Barite and celestite were excluded from future modelling sequence because inhibitors are used by the operator to prevent the formation of these scales. For silicates, it is suspected that kinetic reaction prevents their deposition. That's why they were excluded to focus on the primary elements found in the scales found at the SsF geothermal plant as mentioned before. The results of the calculation are done at the different temperatures (Table 11).

Table 11. Results of refined thermodynamic modelling in weight percentage

		Temperature (°C)								
	M(g/mol)	40	50	60	65	90	120	150	175	200
As	74.922	0.00%	0.00%	0.00%	0.00%	0.00%	0.00%	0.00%	0.00%	0.00%
Cu	63.546	0.04%	0.00%	0.00%	0.00%	0.00%	0.00%	0.00%	0.00%	0.00%
Fe	55.847	45.6%	45.6%	44.8%	45.9%	45.8%	46.2%	46.2%	46.5%	46.4%
Pb	207.2	0.72%	0.50%	1.5%	0.25%	0.52%	0.07%	0.43%	0.04%	0.30%
S	32.066	52.8%	52.9%	52.3%	53.1%	53.0%	53.2%	53.2%	53.4%	53.3%
Sb	121.75	0.77%	1.0%	1.5%	0.76%	0.67%	0.48%	0.17%	0.00%	0.00%

For each step of temperature, the modelling results show that sulfur and iron are the major elements with concentrations of 45% and 53% respectively (table 11). On the other hand, the total amount of the other elements represents less than 3% of the total. Copper is only found at 40°C and in extremely small quantities. Antimony and lead are also found in small quantities (less than 1.5%) at any given step of temperature.

3.2. Kinetic Modelling

The results given out by the calculation of the thermodynamic model gives insight on the precipitation of the minerals at thermodynamic equilibrium which may not necessarily be respected in the conditions studied. Modelling done from a kinetics aspect was proposed and the results from the thermodynamic model were compared and complimented with literature review and field knowledge to select the proper minerals which could precipitate. The kinetic information was mainly obtained from Zhang et al. (2019) [24] as mentioned in the method section. Initially, the model had little modification to the kinetic information used from the source with exception for minerals lacking their kinetic information. Rates equations for metal sulfides including the concentration of oxygen into the calculation are removed because they serve no purpose due to the little to no oxygen content in the brine at the SsF geothermal plant.

For the initial model, two different sets of minerals were considered. The first set of minerals are galena (PbS), orpiment (As_2S_3), pyrite (FeS_2), amorphous silica (SiO_2), quartz(alpha)(SiO_2), and stibnite (Sb_2S_3). Galena and stibnite are known minerals already observed at the SsF plant [15]. Pyrite was considered over arsenopyrite (AsFeS) and chalcopyrite (CuFeS) because pyrite has a higher saturation index than arsenopyrite (Appendix A, Table A1) thus pyrite is more susceptible to precipitate than arsenopyrite. Chalcopyrite was dismissed as the principal provider of Fe precipitation because there is only a small amount of copper found in the analysis done at the SsF plant (Table 2) which is negligeable compared to the quantity of Fe found. As for orpiment, this mineral is the only representative for presence of the element As. For amorphous silica and quartz(alpha), they were considered as they had a major influence in the thermodynamic modelling. Unfortunately, the desired modelling conditions do not fall within the domain of validity

for the initial kinetic model created. For the formation of galena, this model is only valid for a temperature between 25°C to 70°C and a pH between one to three. For the formation of pyrite, this model is only valid for a temperature between 20°c to 40°C and a pH between one to four. For both cases, the range of pH is too acidic compared to the actual case. The model for the formation of orpiment is only valid for a temperature between 25°C to 40°C and a pH between 7.3 to 9.4 which is too alkaline. For the formation of amorphous silica, the model is only valid for a pH around 5.7 which is a bit too alkaline compared to the pH of the fluid at the SsF geothermal plant. For the formation of quartz(alpha), the model is within the proper zone of validity. Regardless, this model was used as an initial approach to modelling the minerals precipitated. For stibnite, no source for its kinetic information aside from its kinetic constant is found [25]. Thus, the kinetic equation of galena was taken and modified to suit the kinetic rate of stibnite. Minerals such as barite and celestite were not added because their exclusion serve as a proxy to their inhibition by chemical treatment.

The second set of minerals consists of the same minerals from the first set but excluding amorphous silica and quartz(alpha). These two minerals were excluded to better focus on the main minerals identified in the scales at the SsF geothermal plant. The modelling with both set of minerals was only done from 200°C to 65°C as it is complicated to model the circulation of fluids in the pipes between the ORC heat exchangers and the test heat exchangers. Furthermore, the residence time and the surface area of the heat exchangers in contact with the brine are different in both cases which will thus further complexify the model. To simplify the model, the ORC heat exchangers was chosen as the standard for the temperature to be modelled.

Table 12. Results for initial kinetics model with first set of minerals in weight percentage

Temperature	Pb	Fe	As	Sb	S	Si	O	Majority
65	8.88%	40.77%	0.14%	1.13%	48.73%	0.16%	0.18%	S
90	2.14%	45.11%	0.01%	0.04%	52.16%	0.24%	0.28%	S
120	0.95%	44.67%	0.00%	0.01%	51.45%	1.4%	1.6%	S
150	0.60%	35.72%	0.00%	0.00%	41.12%	10.5%	12.0%	S
175	0.22%	15.66%	0.00%	0.00%	18.01%	30.9%	35.2%	O
200	0.01%	3.80%	0.00%	0.00%	4.36%	42.9%	48.9%	O

The first results showed that for the temperatures between 65°C to 150°C, S and Fe are the major elements in the simulated scales (Table 12). From 175°C onwards, Si and O are the major elements while Pb, As and Sb are found in negligeable amounts.

Table 13. Results for initial kinetics model with second set of minerals in weight percentage

Temperature	Pb	Fe	As	Sb	S	Majority
65	8.9%	40.9%	0.14%	1.1%	48.9%	S
90	2.2%	45.4%	0.01%	0.04%	52.4%	S
120	0.98%	46.0%	0.00%	0.01%	53.0%	S
150	0.78%	46.1%	0.00%	0.00%	53.1%	S
175	0.64%	46.2%	0.00%	0.00%	53.2%	S
200	0.11%	46.5%	0.00%	0.00%	53.4%	S

The results show that sulfur is the majority for every step of temperature taking up to 53.4% of the composition of scales (Table 13). Iron is shown to be in second largest mass quantity with a weight percentage of around 46% except at 65°C which is at 40.9%. Lead is shown to be in smaller quantity such as 8.9% at 65°C and 2.2% at 90°C respectively. Between 200°C and 120°C, the quantity of lead is less than 1%. As for antimony and arsenic, both are found in extremely small quantities where antimony is at 1.1% and arsenic is at 0.14% for the temperature of 65°C. Antimony and arsenic is not found at higher temperatures (above 150°C).

4. Discussion

4.1. Thermodynamic modelling analysis

The thermodynamic modelling provides insight on possible precipitation of minerals at each temperature step. It can be observed that minerals containing strontium such as celestite were not listed as minerals precipitated by the modelling software (Table 8). In the analysis made on the scales at the SsF plant, traces of strontium were found and were identified to be celestite [7,10]. This discrepancy can be explained by the fact that the supposed mineral found at the plant, celestite dissolves in favor of the precipitation of barite [26]. Since the results are calculated at thermodynamic equilibrium, the total consumption of celestite was already considered during the calculations made by PhreeqC. Another explanation is that the PhreeqC software does not consider the existence of solid solutions like barium/strontium sulfates [7,10-11]. So, the software considers barite over celestite for their precipitation. Thus, strontium was excluded from the comparison of the weight percentage of the elements between the Ssf plant analyses, the thermodynamic models, and the kinetic models. Barite is shown to potentially precipitate at the given range of temperature (Table 8). However, as the temperature decreases, the saturation index of barite increases thus increasing its potential to precipitate (Appendix A, Table A1). A similar situation is observed in the formation of galena, albeit with a higher saturation index. For pyrite, it can also potentially precipitate at the given range of temperature. Its saturation index increases from 200°C to 90°C in which it starts to decrease thereafter. Precipitation of native metals could not be observed in neither thermodynamics modelling nor kinetics modelling because the modelling software cannot take into account their formation.

When silicates were considered for the thermodynamic model, the results (Table 10) showed that Si and O take up the majority of the elements until it rendered the rest of the elements negligeable in the simulated scales. This is not the case at the SsF geothermal plant as there were tiny amounts of silicate in the actual analyses. A second model was constructed by excluding the silicates to have a better focus on the known minerals found at the geothermal plant.

Table 14. Comparison between Soultz-sous-Forêts, thermodynamic model, and kinetic model results in relative percentage by weight

	Temperature	65	90	120	150
Pb	SsF plant analyses	59.7%	56.8%	39.9%	27.3%
	Thermodynamic model 1	0.00%	0.02%	0.00%	0.01%
	Thermodynamic model 2	0.25%	0.52%	0.07%	0.43%
	Kinetic Model 1	8.9%	2.1%	0.95%	0.60%
	Kinetic Model 2	8.9%	2.2%	0.98%	0.78%
Fe	SsF plant analyses	5.9%	12.6%	12.1%	23.3%
	Thermodynamic model 1	0.65%	1.34%	1.37%	1.36%
	Thermodynamic model 2	45.9%	45.8%	46.2%	46.2%
	Kinetic Model 1	40.8%	45.1%	44.7%	35.7%
	Kinetic Model 2	40.9%	45.4%	46.0%	46.1%
As	SsF plant analyses	9%	8%	13%	7%
	Thermodynamic model 1	0%	0%	0%	0%
	Thermodynamic model 2	0.00%	0.00%	0.00%	0.00%
	Kinetic Model 1	0.14%	0.01%	0.00%	0.00%
	Kinetic Model 2	0.14%	0.01%	0.00%	0.00%
Sb	SsF plant analyses	8%	5%	3%	2%
	Thermodynamic model 1	0.01%	0.02%	0.02%	0.01%
	Thermodynamic model 2	0.76%	0.67%	0.48%	0.17%
	Kinetic Model 1	1.13%	0.04%	0.01%	0.00%
	Kinetic Model 2	1.1%	0.04%	0.01%	0.00%
S	SsF plant analyses	17%	18%	32%	41%
	Thermodynamic model 1	1.9%	2.7%	2.9%	2.7%
	Thermodynamic model 2	53.1%	53.0%	53.2%	53.2%
	Kinetic Model 1	48.73%	52.2%	51.5%	41.1%
	Kinetic Model 2	48.9%	52.4%	53.0%	53.1%

The amount of galena formed in the thermodynamic models is greatly inferior to the actual scaling at the SsF geothermal plant (Table 14). There is an unusually high amount of iron and sulfur in the thermodynamic modelling. Furthermore, the quantity of lead is still in the minority. Another problem is that the thermodynamic modelling simulates the precipitation of the minerals over a great amount of time which is until the fluid reaches thermodynamic equilibrium. At the SsF geothermal plant, the precipitation of the minerals is not necessarily at thermodynamic equilibrium since the residence time of the brine in the exchanger is only around three minutes. Furthermore, the initial amount of lead (Pb) (Table 1a) is smaller than the rest of elements in the brine. This could explain the low amount of lead found in simulated scales compared to the other elements in this modelling method. Thus, the thermodynamic model proved to be not sufficient for the prediction of formation of scales at the SsF geothermal plant and kinetic effect must be considered.

4.2. Kinetic modelling analysis

The kinetics model with the first set of minerals (Table 12) showed improvements in the results when compared to the first thermodynamic model (Table 10). The kinetic model with the first set of minerals (Table 12) has significantly reduced the Si and O

contents for the temperatures between 65°C and 150°C. This confirms that the kinetic effect controls the absence of silicates in the SsF scales.

However, for this range of temperature, sulfur (S) and iron (Fe) have the highest concentration with the highest percentage being 52.2% and 45.1% respectively (Table 14). Regardless, the concentration of each element for the kinetic model 1 does not reflect the actual concentration found in the SsF plant analyses.

As for the kinetic model 2, it showed similar improvements in the results to the results of kinetic model 1. At 65°C, the quantity of lead has increased from 0.25 % (thermodynamic model 2) to 8.9% (kinetic model 2) in the composition of elements found in the modelled scales (Table 13). However, iron and sulfur are still the major elements in the modelled scales. The lack of kinetic information on the formation of stibnite could also lead to inaccuracies in the results such as the low amount of antimony. In addition, the amount of sulfur present at each temperature is larger than the actual case. The discrepancies can be explained by the conditions of the modelled scales being outside the domain of validity for temperature and pH of the kinetic information used.

Table 15. Modification of the first kinetic model. n_x: representing the index used in the rates equation (Appendix B)

	Initial model	Modified model
Arsenopyrite	n= 1.68	n= 0.8
Orpiment	n2 = -1.26	n2= -1.48
Stibnite	n= 0.5	n= 0.475
Pyrite	n1= -0.5	n1= -0.25
	n3= 0.5	n3= 0.55

Therefore, to better simulate the scale formation at the SsF geothermal plant, a modified version of the initial model was created. In this second model, the kinetic information of the minerals was modified to reflect closely to the analyses done at the geothermal plant. The kinetic information was purposely modified until the model produces a result similar to the ones obtained at SsF geothermal plant at one temperature step. The modification was done iteratively until the results were in an approximate range of the actual case. Thus, the modified kinetic information is not indicative of any actual kinetic values. The two minerals (arsenopyrite and chalcopyrite) were added to compensate for the low amount of arsenic and the high amount of sulfur and iron. The kinetic information of chalcopyrite is taken from Zhang et al. (2019) whereas no kinetic data was found on arsenopyrite. Thus, the kinetic data of chalcopyrite was taken and modified for arsenopyrite. Next, the kinetic rate of pyrite was slowed down as this mineral has the greatest influence on the increases of percentage of iron and sulfur (Table 15). Overall, the kinetic information of all the minerals except galena and chalcopyrite was modified to obtain a general model for the formation of scales.

Table 16. Mass of elements in percentage for modified kinetics model

Temperature	Pb	Fe	As	Sb	S	Cu	Majority
65	52.2%	5.0%	9.0%	8.5%	22.5%	2.8%	Lead
90	45.6%	16.0%	9.2%	1.2%	25.2%	2.8%	Lead
120	34.9%	23.5%	7.0%	0.42%	29.6%	4.6%	Lead
150	40.1%	22.7%	0.00%	0.01%	32.3%	4.9%	Lead

175	41.7%	23.0%	0.00%	0.00%	32.8%	2.5%	Lead
200	14.4%	38.0%	0.00%	0.00%	45.8%	1.8%	Sulfur

The modified model presented a result that is closer to the analyses of scales at the geothermal plant (Table 14, Table 16). The percentage of sulfur is still higher than the actual case but the increase in quantity of sulfur scales better than the unmodified kinetic information models. The quantity of iron is higher than the actual case for the temperature between 90°C and 150°C. In addition, there are no other minerals that contains antimony and arsenic that has a positive saturation index for temperatures above 120°C. This leads to having small and negligeable quantities of both elements at the mentioned temperature. All things considered, this model allows a rough prediction on the scale formation when operating the plant with sulfate scales inhibitors at the SsF geothermal plant as there is only a small deviation between simulated results and the actual case. The model becomes less accurate at higher temperatures such as at 150°C because of the lack of antimony and arsenic at this temperature (Table 14).

For the modelling of scales for the SsF geothermal plant, a lot of information was lacking such as the kinetic information that is suited for the operating conditions of the plant. Future studies and analyses on the precipitation of the minerals are to be arranged to obtain the missing kinetic information and challenge the modified kinetic model. A laboratory study is necessary to investigate the precipitation of minerals at conditions of the SsF geothermal plant which is at around pH 5.2 and the temperature range of the ORC heat exchangers. The kinetic model for pyrite might also not be suitable for modelling the scales at the pH, pressure, and temperature of SsF geothermal plant which led to inaccuracies in the results pertaining the amount of Fe and S. Therefore, the kinetic information of the precipitation of pyrite as well as galena, arsenopyrite, chalcopyrite, arsenides, sulfosalts, selenides and other base metal sulfides are needed to be determined through this laboratory study so that a proper kinetic model can be constructed.

Furthermore, the inhibition of sulfates such as barium and celestite was just excluded from the calculation due to lack of information on their kinetics. Therefore, the inhibition process should also be analyzed and studied to obtain its kinetic information that can be integrated into the kinetic model. With a proper kinetic model, a more precise result can be obtained through the simulation on the formation of scales in the pipes and exchanger at the geothermal plant. Other than that, other reactions aside from precipitation should also be studied and integrated into the model such as the possibility of heavy metal corrosion in the pipes and heat exchanger as mentioned in Lichti and Brown (2013) [27] and Lichti et al. (2016) [28]. This phenomenon should be studied at the SsF geothermal plant and be verified whether it affects the amount of scales formed at the plant. A study should also be conducted on the possibility of a chemical interaction between FeS and PbS.

5. Conclusions

From the geochemical analyses done on the SsF geothermal plant, lead is found to be the major element in the composition of scales formed when operating the plant with sulfate anti-scales. The principal mineral formed was identified to be galena. This could change when additional chemical treatment is added to the process. To have an accurate prediction on the mineral and elements formed during the scaling phenomenon, a prediction model needs to be created.

The main goal of this study was to better characterize the scales formed at the SsF geothermal plant by establishing a geochemical model that allows the prediction of the formation of scales. Intensive bibliographic research was done to complement the thermodynamic and kinetic information required for the modelling of the formation of scales

at the SsF geothermal plant. The two methods of modelling present their own set of challenges that prevents acquisition of a result that reflects accurately the actual case.

For the thermodynamic modelling, this method is done over a great amount of time which is impractical for predicting the formation of scales in an actual case. The saturation index obtained from thermodynamic modelling however is a good indication on which mineral can precipitate in function of the temperature.

For the kinetic modelling, specific kinetic information such as the rates equation and the kinetic constant for the precipitation of the mineral are lacking for the desired range of temperature. Nevertheless, the modelling shows that silicate precipitation is strongly controlled by kinetic. Additionally, this method allows a more accurate prediction for the formation of scales with the caveat of having the proper kinetic information.

The results obtained in this study open new perspectives on the issue of lack of kinetic information. Bibliographic research was concluded to be insufficient and future laboratory studies, tests and analyses should be done on the precipitation of minerals at the working conditions of the geothermal plant. The scale inhibition should also be analyzed and studied to be integrated into the current model. Laboratory studies should be done to identify any additional reactions that contribute to the formation of scales. The kinetic information obtained from laboratory studies on additional reactions should also be integrated into the current model. With precise kinetic information on the precipitation of the minerals and considering other possible reactions, a more accurate prediction model can be created for future uses.

Author Contributions: Conceptualization, P.K., G.R. and M.D.; methodology, P.K., G.R. and M.D.; software, P.K.; validation, G.R., E.D., M.D., and P.C.; formal analysis, P.K., G.R. and M.D.; investigation, P.K. and G.R.; resources, P.K. and G.R.; data curation, G.R; writing—original draft preparation, P.K. and G.R.; writing—review and editing, P.K., G.R., E.D., M.D., and P.C.; visualization, P.K. and G.R.; supervision, G.R. and M.D.; project administration, G.R., E.D.; funding acquisition, G.R., E.D. All authors have read and agreed to the published version of the manuscript.

Funding: This research was funded by the European Union's Horizon 2020 research and innovation program under grant agreement No 792037 (MEET project).

Acknowledgments: The authors thank the Soultz-sous-Forêts site owner, GEIE Exploitation Minière de la Chaleur, for giving access to their geothermal installation. The authors would also thank Laurent André (BRGM) for the technical support, guidance, and insight on the modelling process. Finally, the author would like to thank Beatrice Ledésert (CY Cergy Paris Université) for providing the microscopic image of the (Pb,As,Sb)S scale found at SsF plant.

Conflicts of Interest: The authors declare no conflict of interest. The funders had no role in the design of the study; in the collection, analyses, or interpretation of data; in the writing of the manuscript, or in the decision to publish the results.

Appendix A

672

Table A1. Saturation Index of minerals with potential to precipitate.

673

Pressure (bar)		**20**								
Temperature (°C)		40	50	60	65	90	120	150	175	200
SiO_2	Amorphous_silica	0.45	0.38	0.32	0.29	0.16	0.03	-0.08	-0.16	-0.24
$CaSO_4$	Anhydrite	-0.98	-0.88	-0.78	-0.73	-0.53	-0.32	-0.1	0.08	0.25
$Cu_{1,75}S$	Anilite	2.61	1.97	1.31	0.97	-0.55	-1.95	-3.05	-3.86	-4.65
FeAsS	Arsenopyrite	-0.52	-0.28	-0.04	0.06	0.3	0.13	-0.24	-0.58	-0.9
$BaSO_4$	Barite	1.24	1.11	0.99	0.93	0.67	0.4	0.21	0.1	0.01
$FeSb_2S_4$	Berthierite	1.33	1.25	1.17	1.13	0.92	0.63	-0.02	-1.48	-3.15
Cu_5FeS_4	Bornite(alpha)	17.03	15.3	13.5	12.59	8.22	3.83	0.17	-2.56	-5.19
SiO_2	Chalcedony	1.16	1.05	0.96	0.91	0.72	0.52	0.34	0.21	0.1
Cu_2S	Chalcocite(alpha)	2.75	2.01	1.24	0.85	-0.89	-2.45	-3.66	-4.53	-5.38
$CuFeS_2$	Chalcopyrite(alpha)	6.21	6.07	5.91	5.8	5.12	4.08	3.01	2.17	1.36
SiO_2	Coesite(alpha)	0.64	0.55	0.47	0.43	0.26	0.09	-0.05	-0.16	-0.26
CuS	Covellite	1.42	1.07	0.71	0.53	-0.36	-1.28	-2.09	-2.7	-3.28
SiO_2	Cristobalite(alpha)	0.89	0.8	0.72	0.68	0.52	0.35	0.21	0.1	0
SiO_2	Cristobalite(beta)	0.83	0.74	0.66	0.62	0.47	0.31	0.17	0.07	-0.02
$Cu_{1,934}S$	Djurleite	2.76	2.05	1.3	0.93	-0.76	-2.29	-3.47	-4.34	-5.18
$Fe_{10}S_{11}$	$Fe_{10}S_{11}$	-19.75	-15.47	-11.34	-9.49	-2.77	0.56	1.65	1.98	2.14
$Fe_{11}S_{12}$	$Fe_{11}S_{12}$	-21.56	-16.83	-12.28	-10.23	-2.81	0.92	2.19	2.61	2.84
$Fe_{7,016}S_8$	$Fe_{7,016}S_8$	-11.61	-8.67	-5.83	-4.55	0.01	2.12	2.67	2.74	2.72
Fe_9S_{10}	Fe_9S_{10}	-16.97	-13.14	-9.45	-7.79	-1.8	1.11	2	2.23	2.31
PbS	Galena	2.57	2.54	2.51	2.49	2.18	1.6	1	0.53	0.05
FeS_2	Marcassite	4.15	4.39	4.63	4.72	4.87	4.42	3.73	3.13	2.56
As_2S_3	Orpiment	0.92	0.97	1.04	1.04	0.58	-0.82	-2.6	-4.1	-5.52
FeS_2	Pyrite	4.84	5.06	5.28	5.36	5.45	4.96	4.23	3.6	3
SiO_2	Quartz(alpha)	1.43	1.31	1.21	1.16	0.95	0.73	0.54	0.4	0.28
SiO_2	Quartz(beta)	1.21	1.11	1.02	0.97	0.78	0.59	0.42	0.29	0.18
$Na_2(Fe_3Fe_2)Si_8O_{22}(OH)_2$	Riebeckite	-7.54	-6.95	-6.34	-6.05	-4.66	-3.17	-1.68	-0.44	0.8
Sb_2S_3	Stibnite	3.25	2.76	2.29	2.08	1.25	0.7	0.02	-1.4	-3.01

674

675

Appendix B

The PhreeqC program can be divided into several parts which signifies different simulation iteration. Every part is ended with the line "End" to carry on to the next simulation. Each part is divided into several sections which has different function when carrying out the calculation for the modelling of fluids. Certain sections are not mandatory for the simulation as each of them serves different purposes. The first section is the "Database" in which we define the database to be use as reference for the calculations. The next section is "Solution" where the properties of the fluid is defined. The properties of the fluids such as the temperature, pressure and pH of the fluid is added to this section. Furthermore, the composition of the fluid is also added to this section. The unit for the concentration of each component in the fluids are also user-defined. In the case of this study, the unit used is in mg/kgw.

The "Gas_Phase" is the next section after the "Solution" section. For this section, it functions similarly as the "Solution" section. In this section, the properties of the gas are defined and the composition in percentage of the gas is declared. The properties of the gas can be modified for the different simulation iterations by using the line "Gas Phase Modify". This section enables the modification of volume, pressure, and the concentration of each component of the gas. In the case of this study, this section is only used to modify the pressure of the gas.

The line "Reaction_Temperature" is used to modify the temperature of the solution after the first simulation iteration. This section allows the modification of the temperature of the fluid to another temperature or to a range of temperature. The line "Equilibrium_Phases" is used to model and simulate the precipitation of minerals. This section allows the user to calculate the number of mole of minerals precipitated or dissolved at thermodynamic equilibrium. The user is required to provide the saturation index of the corresponding minerals at the desired temperature.

The fluid can also be simulated from a kinetic aspect by using the lines "Rates" and "Kinetics". In the "Rates" section, the user is required to provide the rate equation for the given mineral as well as the kinetics constant of the rate equation. The "Kinetics" section then uses the information from the "Rates" section to properly calculate the number of moles of minerals precipitated for a given duration. In this section, the user is required to provide information on the number of moles of minerals present initially in the fluid, the desired duration of the precipitation of the minerals, the number of intervals between the given duration and the type of Runge Kutta equation used. The Runge Kutta method is a family of implicit and explicit iterative methods that includes the Euler method. This method is used in temporal discretization for the approximate solution of differential equations.

The final command line used in the current study is the "Selected_Output" command line. This section allows the user to output the certain parts of the results of the simulation into a text fil or a csv file.

```
DATABASE C:\phreeqc\database\PHREEQC_ThermoddemV1.10_15Dec2020.dat
SOLUTION 1
    Units mg/L
    Temperature 25.0
    Pressure  1.0
    pH  5.2

    Cl  55942
    Na  26412
    Ca  7018
```

```
        K   3357
        S   64.4
        Pb   0.113
        Sr   422.415
        Ba   25.55
        Sb   0.0645
        As   9.676
        Fe   26.3
        Si   179
        Cu   0.001

GAS_PHASE 1
        -Pressure 1.0
        -Fixed_Pressure
        -Temperature 25
        -Volume 1.03
        CO2(g)          0.882
        N2(g)           0.0908
        CH4(g)          0.0239
END
USE SOLUTION 1
USE GAS_PHASE 1

GAS_PHASE_MODIFY 1
Pressure    19.7385

RATES

################
#arsenopyrite
################


-start
1 rem assuming Fe(III)>1e-4M is the switch point for Fe-promoted mechanism
10 R=8.31451
20 if TOT("Fe(3)")<=1e-4 then J=(10^-1.52)*EXP(-28200/(R*TK))*ACT("H+")^0.8
30 if (parm(1)>0) then SA0=parm(1) else SA0=1
40 if (M0<=0) then SA=SA0 else SA=SA0* (M/M0)^0.67
70 SR_mineral=SR("Arsenopyrite")
80 if (M<0) then goto 150
90 if (M=0 and SR_mineral<1) then goto 150
100 rate=J*SA*(1-SR_mineral) *parm(2)
120 moles=rate*Time
150 Save moles
-end

################
# chalcopyrite (Kimball et al 2010)
################
chalcopyrite(alpha)

# experimental condition range T=4-100C, pH=0-5, log C(Fe+++)=-5-0
```

```
-start
1 rem assuming Fe(III)>1e-4M is the switch point for Fe-promoted mechanism
10 R=8.31451
20 if TOT("Fe(3)")<=1e-4 then J=(10^-1.52)*EXP(-28200/(R*TK))*ACT("H+")^1.68 else
J=(10^1.88)*EXP(-
    48100/(R*TK))*ACT("H+")^0.8*TOT("Fe(3)")^0.42
30 if (parm(1)>0) then SA0=parm(1) else SA0=1
40 if (M0<=0) then SA=SA0 else SA=SA0* (M/M0)^0.67
70 SR_mineral=SR("Chalcopyrite(alpha)")
80 if (M<0) then goto 150
90 if (M=0 and SR_mineral<1) then goto 150
100 rate=J*SA*(1-SR_mineral)*parm(2)
120 moles=rate*Time
150 Save moles
-end

################
# Galena (Acero et al, 2007)
################
Galena

# experimental condition range T=25-70C, pH=1-3

-start
1 rem unit should be mol, kgw-1 and second-1
2 rem parm(1) is surface area in the unit of m2/kgw
3 rem calculation of surface area can be found in the note
4 rem M is current moles of minerals
5 rem M0 is the initial moles of minerals
6 rem parm(2) is a correction factor
40 SR_mineral=SR("Galena")
41 if (M<0) then goto 200
42 if (M=0 and SR_mineral<1) then goto 200
43 if (M0<=0) then SA=PARM(1) else SA=PARM(1)*(M/M0)^0.67
50 if (SA<=0) then SA=1
60 R=8.31451
70 J=10^-5.7*exp(-23000/R/TK)*ACT("H+")^0.43
90 Rate=J*(1-Sr_mineral)*SA*parm(2)
100 moles=Rate*Time
200 save moles
-end


###########
#As2S3(a)
###########
Orpiment

# from Palandri and Kharaka 2004
# experimental condition range T=25-40C, pH=7.3-9.4

-start
```

```
1 rem unit should be mol,kgw-1 and second-1
2 rem parm(1) is surface area in the unit of m2/kgw
3 rem calculation of surface area can be found in the note
4 rem M is current moles of minerals. M0 is the initial moles of minerals
5 rem parm(2) is a correction factor
10 rem acid solution parameters
11 a1=0
12 E1=0
13 n1=0
20 rem neutral solution parameters
21 a2=4.95E-09
22 E2=8700
23 n3=0.180
30 rem base solution parameters
31 a3=1.36E-16
32 E3=8700
33 n2=-1.48
36 rem rate=0 if no minerals and undersaturated
40 SR_mineral=SR("ORPIMENT")
41 if (M<0) then goto 200
42 if (M=0 and SR_mineral<1) then goto 200
43 if (M0<=0) then SA=PARM(1) else SA=PARM(1)*(M/M0)^0.67
50 if (SA<=0) then SA=1
60 R=8.31451
75 Rate1=a1*EXP(-E1/R/TK)*ACT("H+")^n1    #acid rate expression
80 Rate2=a2*EXP(-E2/R/TK)*ACT("O2")^n3                    #neutral rate expression
85 Rate3=a3*EXP(-E3/R/TK)*ACT("H+")^n2      #base rate expression
90 Rate=(Rate1+Rate3)*(1-Sr_mineral)*SA*parm(2)
100 moles= rate*Time
200 save moles
-end

###############
#pyrite
############
pyrite
# from Palandri and Kharaka 2004
# experimental condition range T=20-40C, pH=1-4

-start
1 rem unit should be mol,kgw-1 and second-1
2 rem parm(1) is surface area in the unit of m2/kgw
3 rem calculation of surface area can be found in the note
4 rem M is current moles of minerals. M0 is the initial moles of minerals
5 rem parm(2) is a correction factor
10 rem acid solution parameters
11 a1=2.82E+02
12 E1=56900
13 n1=-0.25
14 n3=0.55
30 rem neutral solution parameters
31 a3=2.64E+05
32 E3=56900
```

```
33 n2=0.500
36 rem rate=0 if no minerals and undersaturated
40 SR_mineral=SR("pyrite")
41 if (M<0) then goto 200
42 if (M=0 and SR_mineral<1) then goto 200
43 if (M0<=0) then SA=PARM(1) else SA=PARM(1)*(M/M0)^0.67
50 if (SA<=0) then SA=1
60 R=8.31451
75 Rate1=a1*EXP(-E1/R/TK)*ACT("H+")^n1*ACT("Fe+3")^n3    #acid rate expression
80 Rate2=a2*EXP(-E2/R/TK)*ACT("O2")                      #neutral rate expression
90 Rate=(Rate1)*(1-Sr_mineral)*SA*parm(2)
100 moles= rate*Time
200 save moles
-end

Stibnite
-start

1 rem unit should be mol,kgw-1 and second-1
2 rem parm(1) is surface area in the unit of m2/k     g       w
3 rem calculation of surface area can be found in the note
4 rem M is current moles of minerals
5 rem M0 is the initial moles of minerals
6 rem parm(2) is a correction factor
40 SR_mineral= SR("Stibnite")
41 if (M<0) then goto 200
42 if (M=0 and SR_mineral<1) then goto 200
43 if (M0<=0) then SA=PARM(1) else SA=PARM(1)*(M/M0)^0.67
50 if (SA<=0) then SA=1
60 k=1.25E-10*EXP(298.2/TK)
70 J=k*ACT("H+")^0.475
90 Rate=J*(1-SR_mineral)*SA*parm(2)
100 moles=Rate*Time
200 save moles
-end

KINETICS

    Arsenopyrite
        -M    0.0
        -M0   0.0
        -parms      1.0    1.0
        -tol    1e-8
    -steps 1 minute
    -step_divide 10
    -runge_kutta 3

    Chalcopyrite(alpha)
        -M    0.0
        -M0   0.0
        -parms      1.0    1.0
        -tol    1e-8
    -steps 1 minute
```

```
    -step_divide 10
    -runge_kutta 3

    Galena
        -M    0.0
        -M0   0.0
        -parms    1.0    1.0
        -tol    1e-8
    -steps 1 minute
    -step_divide 10
    -runge_kutta 3

    Orpiment
        -M    0.0
        -M0   0.0
        -parms    1.0    1.0
        -tol    1e-8
    -steps 1 minute
    -step_divide 10
    -runge_kutta 3

    Pyrite
        -M    0.0
        -M0   0.0
        -parms    1.0    1.0
        -tol    1e-8
    -steps 1 minute
    -step_divide 10
    -runge_kutta 3

    Stibnite
        -M    0.0
        -M0   0.0
        -parms    1.0    1.0
        -tol    1e-8
    -steps 1 minute
    -step_divide 10
    -runge_kutta 3


REACTION_TEMPERATURE 1
    40.0 50.0 60.0 65.0 90.0 120.0 150.0 175.0 200.0

EQUILIBRIUM_PHASES
40°C
Amorphous_silica    0.45    0.0
Barite              1.24    0.0
Chalcedony          1.16    0.0
Coesite(alpha)      0.64    0.0
Cristobalite(alpha) 0.89    0.0
```

Cristobalite(beta)	0.83	0.0
Quartz(alpha)	1.43	0.0
Quartz(beta)	1.21	0.0
Anilite	2.61	0.0
Berthierite	1.33	0.0
Bornite(alpha)	17.03	0.0
Chalcocite(alpha)	2.75	0.0
Chalcopyrite(alpha)	6.21	0.0
Covellite	1.42	0.0
Djurleite	2.76	0.0
Galena	2.57	0.0
Marcassite	4.15	0.0
Orpiment	0.92	0.0
Pyrite	4.84	0.0
Stibnite	3.25	0.0

References

1. Genter, A.; Evans, K.; Cuenot, N.; Fritsch, D.; Sanjuan, B. Contribution of the exploration of deep crystalline fractured reservoir of Soultz to the knowledge of enhanced geothermal systems (EGS). Comptes Rendus Geoscience (2010), 342, 502–516.
2. Vidal, J.; Genter, A. Overview of naturally permeable fractured reservoirs in the Upper Rhine Graben: Insights from geothermal wells. Geothermics (2018), 74, 57-73.
3. Schill, E.; Genter, A.; Cuenot, N.; Kohl, T. Hydraulic performance history at the Soultz EGS reservoirs from stimulation and long-term circulation tests. Geothermics (2017), 70, 110-124.
4. Baujard, C.; Genter, A.; Cuenot, N.; Mouchot, J.; Maurer, V.; Hehn, R.; Ravier, G.; Seibel, O.; Vidal, J. Experience Learnt from a Successful Soft Stimulation and Operational Feedback after 2 Years of Geothermal Power and Heat Production in Rittershoffen and Soultz-sous-Forêts Plants (Alsace, France). GRC Transactions (2018), 42.
5. Mouchot, J.; Ravier, G.; Seibel, O.; Pratiwi, A. Deep Geothermal Plants Operation in Upper Rhine Graben: Lessons Learned. Proceedings, European Geothermal Congress, Den Haag, The Netherlands, 11-14 June 2019.
6. Scheiber, J.; Nitschke, F.; Seibt, A.; Genter, A. Geochemical and Mineralogical Monitoring of the Geothermal Power Plant in Soultz-sous-Forêts (France). Proceedings, 37th Workshop on Geothermal Reservoir Engineering, Stanford University, Stanford, California, USA, January 30 - February 1, 2012.
7. Haas-Nüesch, R.; Heberling, F.; Schild, D.; Rothe, J.; Dardenne, K.; Jähnichen, S.; Eiche, E.; Marquardt, C.; Metz, V.; Schäfer, T. Mineralogical characterization of scalings formed in geothermal sites in the Upper Rhine Graben before and after the application of sulfate inhibitors. Geothermics (2018), 71, 264-273.
8. Mouchot, J.; Cuenot, N.; Bosia, C.; Genter, A.; Seibel, O.; Ravier, G.; Scheiber, J. First year of operation from EGS geothermal plants in Alsace, France: scaling issues. Proceedings, 43rd Workshop on Geothermal Reservoir Engineering, Stanford University, Stanford, California, USA, February 12-14, 2018.
9. Sanjuan, B. "Soultz EGS pilot plant exploitation - Phase III: Scientific program about on-site operations of geochemical monitoring and tracing (2010-2013)". First yearly progress report BRGM/RP-59902-FR (2011), 92 p.
10. Nitschke, F. Geochemische Charakterisierung des geothermalen Fluids und der damit verbundenen Scalings in der Geothermieanlage Soultz sous Forêts, Masterthesis, Institut für Mineralogie und Geochemie (IMG) at Karlsruher Institut of Technology (KIT). (2012), 126 pp.
11. Sanjuan, B.; Rose, P.; Gérard, A.; Brach, M.; Crouzet, C.; Touzelet, S.; Charlot, A. Geochemical monitoring at Soultz-sous-Forêts (France) between October 2006 and March 2007, after the chemical stimulations (RMA, NTA and OCA) carried out in the wells GPK-4 and GPK-3. In: Proceedings of the EHDRA (2007).
12. Portier, S.; Vuataz, F.-D.; Nami, P.; Sanjuan, B.; Gérard, A. Chemical stimulation techniques for geothermal wells: experiments on the 3-well EGS system at Soultz-sous-Forêts. Geothermics (2009), 38, 349–359.
13. Gentier, S.-; Sanjuan, B. ; Rachez, X. ; Tran Ngoc, T. D. ; Beny, C. ; Peter-Borie, M. ; Souque, C.; A progress in the comprehension of fluid circulation in the site of Soultzsous- Forêts: BRGM contribution to the STREP "EGS Pilot Plant". Final Report BRGM/RP-57437-FR, BRGM, Orléans, France 2009, p. 97.
14. Ledésert, B.A; Hébert, R.L.; Mouchot, J.; Bosia, C.; Ravier, G.; Seibel, O.; Dalmais, E.; Ledésert, M.; Trullenque, G.; Sengelen, X.; Genter, A. Scaling in a Geothermal Heat Exchanger at Soultz-sous-Forets (Upper Rhine Graben, France): A XRD and SEM-EDS Characterization of Sulfide Precipitates, Geosciences (2021a), 11,271.

15. Seibel, O.; Mouchot, J.; Ravier, G.; Ledésert, B.; Sengelen, X.; Hebert, R; Ragnarsdótti, K. R., Ólafsson, D.I.; Haraldsdóttir, H.Ó. Optimised valorisation of the geothermal resources for EGS plants in the Upper Rhine Graben. Proceedings, World Geothermal Congress 2020+1, Reykjavik, Iceland, March - October 2021.
16. Gifaut, E.; Grivé, M.; Blanc, P.; Vieillard, P.; Colàs, E.; Gailhanou, H.; Gaboreau, S.; Marty, N.; Madé, B.; Duro, L. Andra thermodynamic database for performance assessment: thermoChimie. Appl Geochem. (2014); 49:225–36.
17. Moog, H.C.; Bok, F.; Marquardt, C.M.; Brendler, V. Disposal of nuclear waste in host rock formations featuring high-saline solutions—implementation of a thermodynamic reference database (THEREDA). Appl Geochem. (2015); 55:72–84.
18. Parkhurst, D.L.; Appelo, C.A.J. Description of input and examples for PHREEQC version 3—A computer program for speciation, batch-reaction, one-dimensional transport, and inverse geochemical calculations: U.S. Geological Survey Techniques and Methods (2013), book 6, chap. A43, 497 p., available only at http://pubs.usgs.gov/tm/06/a43/.
19. Bosia, C.; Mouchot, J.; Ravier, G.; Seibt, A.; Jähnichen, S.; Degering, D.; Scheiber, J.; Dalmais, E.; Baujard, C.; Genter, A. Evolution of Brine Geochemical Composition during Operation of EGS Geothermal Plants (Alsace, France). Proceedings, 46th Workshop on Geothermal Reservoir Engineering, Stanford University, Stanford, California, February 15 - 17 2021.
20. Blanc, P., Lassin, A., Piantone, P., Azaroual, M., Jacquemet, N., Fabbri, A., Gaucher, E.C. Thermoddem: A geochemical database focused on low temperature water/rock interactions and waste materials. Appl. Geochem 2012. 27, 2107–2116.
21. Delany, J.M., Lundeen, S.R. The LLNL Thermochemical Data Base – Revised Data and File Format for the EQ3/6 Package. (1991).
22. Langmuir, D. Aqueous environmental geochemistry. Prentice Hall (1997).
23. Hettkamp, T.; Baumgaertner, J.; Paredes, R.; Ravier, G.; Seibel, O. Industrial Experiences with Downhole Geothermal Line-Shaft Production Pumps in Hostile Environment in the Upper Rhine Valley. Proceedings, World Geothermal Congress 2020+1, Reykjavik, April - October Iceland (2021).
24. Zhang, Y.; Hu, B.; Teng, Y.; Tu, Kevin.; Zhu, C. A library of BASIC scripts of reaction rates for geochemical modeling using PHREEQC. Computer & Geoscience (2019), volume 133. Available online : https://github.com/HydrogeoIU/PHREEQC-Kinetic-Library/blob/master/PHREEQC%20script.txt
25. Biver, M.; Shotyk, W. Stibnite (Sb2S3) oxidative dissolution kinetics from pH 1 to 11. Geochimica et Cosmochimica Acta 79 (2012), 127–139.
26. Poonoosamya, J.; Curti, E.; Kosakowski, G.; Grolimund, D.; Van Loon, L.R.; and Mäder, U. Barite precipitation following celestite dissolution in a porous medium: A SEM/BSE and μ-XRD/XRF study. Geochimica et Cosmochimica Acta (2016), 182, Pg 131-144
27. Lichti, K. A.; Brown, K. L. Prediction and Monitoring of Scaling and Corrosion in pH Adjusted Geothermal Brine Solutions. NACE International Corrosion Conference & Expo 2013.
28. Lichti, K. A.; Ko, M.; Kennedy, J. Heavy Metal Galvanic Corrosion of Carbon Steel in Geothermal Brines. NACE International Corrosion Conference & Expo 2016.

Imprint

Project Lead	ES-Géothermie 26 boulevard du Président Wilson 67932 Strasbourg Cedex 9, FRANCE https://geothermie.es.fr/en/	
Project Coordinator	Dr Albert Genter albert.genter@es.fr	Eléonore Dalmais eleonore.dalmais@es.fr
Scientific Manager	Dr Ghislain Trullenque Ghislain.TRULLENQUE@unilasalle.fr	
Project Manager	Dr Jean Herisson jherisson@ayming.com	
Project Website	https://www.meet-h2020.com/	
LinkedIn page	https://www.linkedin.com/in/meet-eu-project/	

Report Authorship: DALMAIS E., JESTIN C., MAURER V., KUNAN P., (2021). Summary of chemical and physical tests for colder reinjection, MEET report, Deliverable D3.10, September 2021, 64 pp.

Liability claim